8-2019

# Transport and Distribution of Bovine Milk Exosomes and miR-34a Cargo in Murine Cerebral Cortex Endothelial bEnd.3 Cells and BV2 Microglia

Pearl Ebea
*University of Nebraska-Lincoln*, pebea@huskers.unl.edu

# TRANSPORT AND DISTRIBUTION OF BOVINE MILK EXOSOMES AND MIR-34A CARGO IN MURINE CEREBRAL CORTEX ENDOTHELIAL BEND.3 CELLS AND BV2 MICROGLIA

by

Pearl Onuwa Ebea

A THESIS

Presented to the Faculty of
The Graduate College at the University of Nebraska
In Partial Fulfillment of Requirements
For the Degree of Master of Science

Major: Nutrition

Under the Supervision of Professor Janos Zempleni

Lincoln, Nebraska

August, 2019

# TRANSPORT AND DISTRIBUTION OF BOVINE MILK EXOSOMES AND MIR-34A CARGO IN MURINE CEREBRAL CORTEX ENDOTHELIAL BEND.3 CELLS AND BV2 MICROGLIA

Pearl Onuwa Ebea, M.S.

University of Nebraska, 2019

Advisor: Janos Zempleni

The blood-brain barrier (BBB) poses an obstacle in the delivery of drugs to the brain. Bovine milk exosomes (BME) are explored for delivering antisense oligonucleotides to tumors, because BME are bioavailable and protect RNA cargos against degradation in the gastrointestinal tract. This study had the following objectives: 1) assess the transport kinetics of BME and their RNA cargos and secretion of RNA across the apical membrane in murine cerebral cortex endothelial bEnd.3 cells and 2) determine whether murine brain BV2 microglia have the potential to accumulate and, therefore, eliminate BME that crossed the BBB. The uptake of BME labeled with a lipophilic membrane dye followed Michaelis-Menten kinetics in bEnd.3 cells: $V_{max}$ = 0.77 ± 0.20 x $10^{11}$ BME/(10,000 cells x 45 min); $K_m$ = 1.8 ± 2.2 x $10^{11}$ BME/mL. Transport kinetics were similar in BV2 microglia compared to bEnd.3 cells. When BME were labeled with an RNA-reactive dye and uptake was analyzed by using Z-stack confocal microscopy, it was apparent that BME entered the cytoplasm of bEnd.3 cells. Studies of BME transfected with fluorophore-labeled miR-34a suggested that detectable amounts of miR-34a were transported from the apical into the basolateral compartment in dual chamber systems. We conclude that BME deserve further exploration for drug delivery across the BBB.

**ACKNOWLEDGEMENT**

Firstly, I will like to extend my gratitude to my advisor, Dr. Janos Zempleni, for giving me this unique opportunity to join the University of Nebraska-Lincoln and to grow as a member of his lab. I am thankful for his continuous efforts to instill in me valuable knowledge to help my scientific growth and for providing me with resources to succeed on my path. I will also like to thank my committee members – Dr. Sarath Gautam and Dr. Jiujiu Yu for their support and valuable advice throughout my program.

I will like to thank our former laboratory technician – David Giraud, who provided valuable and timely technical assistance to keep my projects running smoothly, as well as our current technician - Yilin Liu who is ever so kind and concerned. I acknowledge and appreciate my colleagues in the lab, particularly Sonal Sukreet and Bijaya Upadhyaya – for teaching me essential experimental methods and guiding me throughout my program, as well as Afsana Khanam, Ezra Mutai, Fang Zhou, Di Wu, Mahrou Sadri, Deborah Fratantonio, Sonia Manca, Wei Zhao and Shu Wang. They have been great sources of support and encouragement within and outside the lab. With much appreciation, I also acknowledge the NHS administrative staff – Diane Nelson, Diane Brown, Amy Brown, Sarah Gibson and Lori Rausch and our department chair, Dr. Mary Ann Johnson.

Lastly, I express my utmost gratitude to my ever-supportive family and my dear friends for their love, prayers and best wishes for me throughout my MS program at the University of Nebraska-Lincoln.

Pearl Onuwa Ebea

August, 2019

# TABLE OF CONTENTS

# LIST OF FIGURES

CHAPTER ONE



CHAPTER TWO

# CHAPTER ONE
# LITERATURE REVIEW

**Extracellular vesicles**

The term extracellular vesicles (EVs) refers to the various types of membrane-bound vesicles secreted by virtually all cell types including prokaryotes and eukaryotes. As determined by their biogenesis, size, morphology and content, extracellular vesicles have been broadly classified into 3 sub-groups: exosomes, microvesicles and apoptotic bodies [1] and more recently classified into two classes: exosomes and microvesicles [2]. Although, previously considered as waste products from cells [3], EVs particularly exosomes, are now better understood to play critical roles in cell-to-cell communication. A number of mechanisms by which EVs are taken up by recipient cells have been proposed through studies using inhibitors of specific pathways, antibodies and knockdown experiments, these proposed mechanisms include fusion of EVs with plasma membrane of cells, clathrin and caveolin mediated endocytosis, phagocytosis and macropinocytosis (Figure 1.1) [4]. In addition, the specific proteins displayed by EVs provide information about their cell type of origin, fate and function [2].

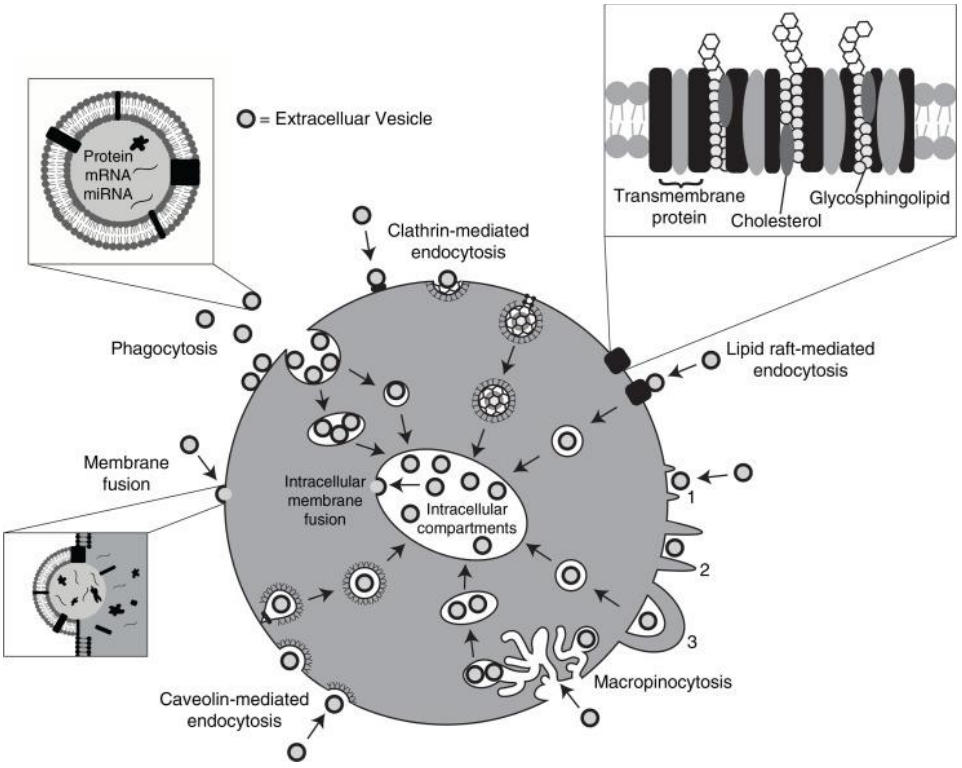


Figure 1.1 Proposed mechanisms of EV uptake by recipient cells. Adapted from Mulcahy et al., 2014 [4].

**Exosomes and RNAs**

Exosomes are nano-vesicles of 30 nm - 100 nm in size that are formed by the inward budding of the plasma membrane, which gives rise to the early endosome. The process of early and late endosome maturation leads to the formation of multivesicular bodies that fuse to the plasma membranes to release the enclosed intraluminal vesicles which are then called exosomes [5, 6] (Figure 1.2). Exosomes contain various cargos such as nucleic acids, lipids and proteins and can be considered the most biological significant class of EVs because of their critical role in protecting and transporting these labile cargos through endocytosis of exosomes into recipient cells [7, 8]. Also noteworthy is the knowledge that loading of RNA cargos into exosomes involves nonrandom sorting mechanisms [9]. These features make exosomes appealing vehicles for targeted delivery of drugs and biomolecules for which they are currently being extensively

studied [10-12]. Naturally occurring exosomes found in bovine milk show great potential as a scalable source for biomolecule delivery due to their size, biocompatibility, safety and cost-effectiveness making them advantageous over synthetic nanoparticle formulations [12]. Mature microRNAs are short non-coding RNAs (approximately 22 nucleotides long) that regulate gene expression by pairing with 3' untranslated regions (UTR) of target mRNAs. Perfect complementarity between the miRNA and target mRNA leads to mRNA degradation whereas partial complementarity leads to inhibition of translation [13-15]. The regulation of genes by miRNAs has been implicated in numerous physiological and pathological conditions in humans such as cancer, cardiovascular diseases, schizophrenia, diabetes and obesity [16-22]. MiRNAs in exosomes have been studied and reports suggest that manipulating exosomal miRNAs ex vivo may be an efficient tool to deliver miRNAs to target specific organs [10, 23]. Our research group discovered that miRNA cargos present in bovine milk are bioavailable to humans and other non-bovine species and can regulate genes and metabolism in these species [7, 8, 24]. Related studies also demonstrated that miRNA cargos in BME accumulate primarily in the intestinal mucosa, liver, spleen and brain when administered to mice [25], and that depletion of milk exosomes and RNA from mice diets affect sensorimotor gating and cognitive performance in mice such as spatial learning and memory [26]. Also, it was recently observed that a significant amount of microbial RNAs are present in BME and ongoing studies suggest that these are bioavailable in mice and humans and possess biological activity therein (Wu et al., unpublished).

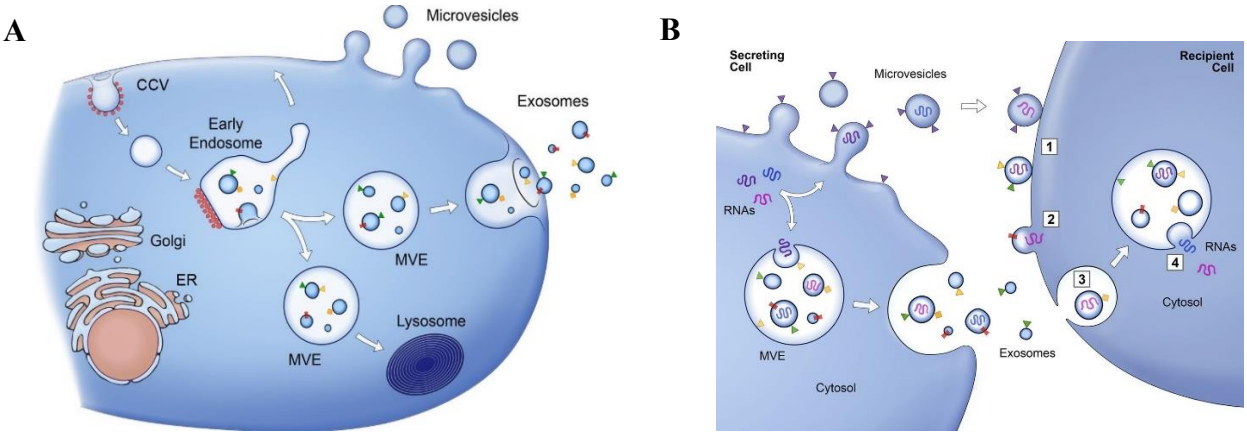


Figure 1. 2 Exosome biogenesis and release from the plasma membrane of cells. (A) Intraluminal vesicles contained in MVEs fuse with the plasma membrane of the cell; (B) releasing its contents (now exosomes) to the neighboring cell. Adapted from Raposo et al., 2013 [27].

**The Blood-Brain Barrier (BBB)**

The BBB is a highly selectively permeable barrier that line the blood vessels in the brain. It plays a critical role in the maintenance of homeostasis in the central nervous system by preventing the entry of potentially harmful compounds while allowing passage of required nutrients into the brain and efflux of waste products. The BBB also protects the brain from changes in ionic composition that occur during daily activities [28]. It is formed primarily by the brain endothelial cells that line the cerebral capillaries with support from astrocytes and pericytes in the brain (Figure 1.3). These endothelial cells possess unique properties that support their function including complex tight junctions formed by transmembrane proteins (e.g. occludin, claudins and junctional adhesion molecules) and adaptor proteins such as zonula occludens protein 1 (ZO-1). [28, 29].

Astrocytes have also been shown to possess significant function in upregulating BBB features such as expression of tight junctions (physical barrier), polarized localization of transporters (transport barrier) and enzyme systems function (metabolic barrier) [28, 29]. Another important

cell type of the central nervous system (CNS) are the microglia. These cells are referred to as the resident macrophages of the CNS, playing a crucial role in the active immune system in the brain by eliminating cell debris, dead cells and other foreign compounds and particles thereby preventing infection and inflammation in the CNS. They also play a role in normal CNS development and maintenance. Of note, they are markedly different from macrophages of peripheral tissues due to their highly sensitive nature and ability to respond rapidly to very subtle changes in the brain microenvironment [30, 31]. In recent years however, microglia have been seen as mediators of neuroinflammation and their dysregulation has been implicated in neurodegenerative diseases and brain cancers [31, 32].

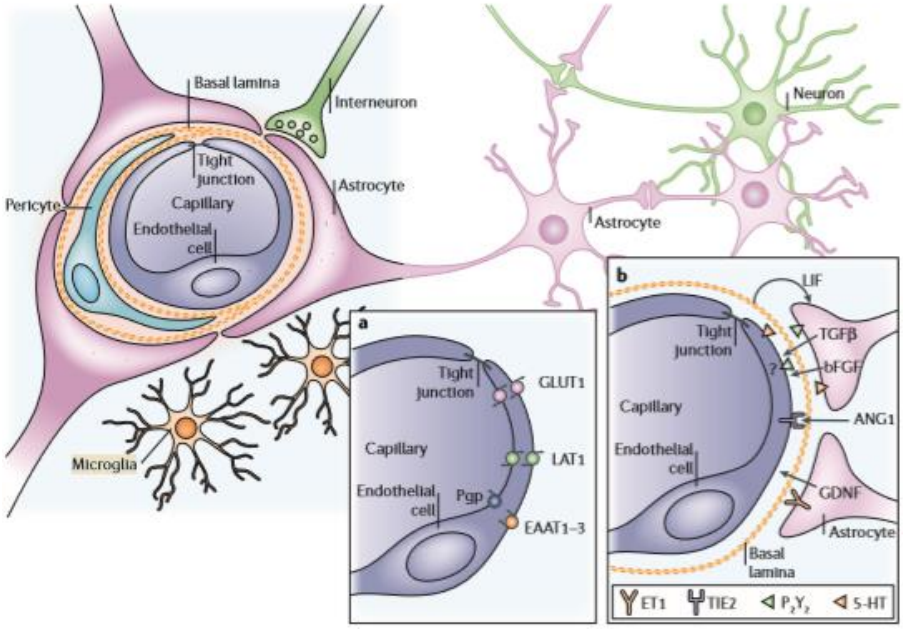


Figure 1. 3 Cellular components of the blood-brain barrier (BBB) are shown including closely associated cell types, transporters and receptors as well as inducing factors. EAAT1–3, excitatory amino acid transporters 1–3; GLUT1, glucose transporter 1; LAT1, L-system for large neutral amino acids; Pgp, P-glycoprotein. 5-HT, 5-hydroxytryptamine (serotonin); ANG1, angiopoetin 1; bFGF, basic fibroblast growth factor; ET1, endothelin 1; GDNF, glial cell line-

derived neurotrophic factor; LIF, leukemia inhibitory factor; P2Y2, purinergic receptor; TGFβ, transforming growth factor-β; TIE2, endothelium-specific receptor tyrosine kinase 2. Adapted from Abbott et al., 2006 [28].

**Methods of assessing transport across the BBB**

The BBB structure and function has been the focus of many studies because it prevents successful delivery of therapeutically relevant amounts of drugs to the brain, thereby blocking the development of neuropharmaceuticals for the treatment of brain related diseases [29, 33]. As a result, several methods have been developed to assess BBB function and the transport of molecules across the BBB in normal and pathological conditions. These include the use of in vivo approaches such as intravenous injections, brain perfusion methods, positron emission tomography, single-photon emission computed tomography and serial two-photon tomography, while in vitro studies include the use of two-dimensional (2-D) transwell systems and three-dimensional (3-D) systems (extracellular matrix (ECM)-based models, spheroidal models and microfluidic models), details of which have been discussed in these articles [34-36]. Transwell-systems are a widely used model of the BBB, in which monolayers of brain endothelial cells are cultured on apical side of membrane-coated inserts and astrocytes and/or pericytes are cultured underneath inserts or in the bottom of multi-well plates (Figure 1.4). Although, it lacks the intact in-vivo organization of components of the BBB, this system has been used for its time and cost effectiveness, ease of maintenance and is recommended for application in in vitro transport and permeability studies [35].

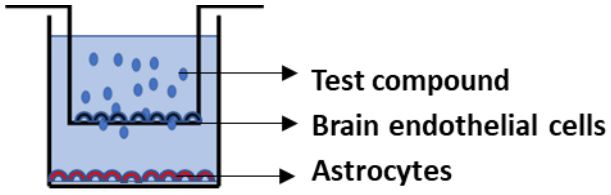


Figure 1. 4 Schematic representation of a 2-D co-culture transwell system showing endothelial cells on apical inserts and astrocytes in the basolateral chamber.

**REFERENCES**


1. Yanez-Mo, M., et al., *Biological properties of extracellular vesicles and their physiological functions.* J. Extracell. Vesicles, 2015. **4**: p. 27066.
2. van Niel, G., G. D'Angelo, and G. Raposo, *Shedding light on the cell biology of extracellular vesicles.* Nat Rev Mol Cell Biol, 2018. **19**(4): p. 213-228.
3. Nagarajah, S., *Exosome secretion—more than simple waste disposal? Implications for physiology, diagnostics and therapeutics.* Journal of circulating biomarkers, 2016. **5**: p. 7.
4. Mulcahy, L.A., R.C. Pink, and D.R. Carter, *Routes and mechanisms of extracellular vesicle uptake.* J. Extracell. Vesicles, 2014. **3**.
5. Simons, M. and G. Raposo, *Exosomes--vesicular carriers for intercellular communication.* Curr. Opin. Cell Biol., 2009. **21**(4): p. 575-581.
6. Mathivanan, S., H. Ji, and R.J. Simpson, *Exosomes: extracellular organelles important in intercellular communication.* J Proteomics, 2010. **73**(10): p. 1907-20.
7. Baier, S.R., et al., *MicroRNAs are absorbed in biologically meaningful amounts from nutritionally relevant doses of cow's milk and affect gene expression in peripheral blood mononuclear cells, HEK-293 kidney cell cultures, and mouse livers.* J. Nutr., 2014. **144**: p. 1495-1500.
8. Wolf, T., S.R. Baier, and J. Zempleni, *The intestinal transport of bovine milk exosomes is mediated by endocytosis in human colon carcinoma caco-2 cells and rat small intestinal IEC-6 cells.* J. Nutr., 2015. **145**: p. 2201-2206.
9. Squadrito, M.L., et al., *Endogenous RNAs Modulate MicroRNA Sorting to Exosomes and Transfer to Acceptor Cells.* Cell Rep., 2014. **8**(5): p. 1432-1446.

10. Alvarez-Erviti, L., et al., *Delivery of siRNA to the mouse brain by systemic injection of targeted exosomes.* Nat Biotechnol, 2011. **29**(4): p. 341-5.

11. Luan, X., et al., *Engineering exosomes as refined biological nanoplatforms for drug delivery.* Acta Pharmacologica Sinica, 2017. **38**(6): p. 754.

12. Munagala, R., et al., *Bovine milk-derived exosomes for drug delivery.* Cancer Lett., 2016. **371**(1): p. 48-61.

13. Chen, K. and N. Rajewsky, *The evolution of gene regulation by transcription factors and microRNAs.* Nat. Rev. Genet., 2007. **8**(2): p. 93-103.

14. Jing, Q., et al., *Involvement of microRNA in AU-rich element-mediated mRNA instability.* Cell, 2005. **120**(5): p. 623-634.

15. Djuranovic, S., A. Nahvi, and R. Green, *miRNA-mediated gene silencing by translational repression followed by mRNA deadenylation and decay.* Science, 2012. **336**(6078): p. 237-240.

16. Hu, G., K.M. Drescher, and X. Chen, *Exosomal miRNAs: biological properties and therapeutic potential.* Frontiers in genetics, 2012. **3**: p. 56.

17. Danielson, K.M. and S. Das, *Extracellular Vesicles in Heart Disease: Excitement for the Future?* Exosomes Microvesicles, 2014. **2**: p. 1.

18. Vojtech, L., et al., *Exosomes in human semen carry a distinctive repertoire of small non-coding RNAs with potential regulatory functions.* Nucleic Acids Res., 2014. **42**(11): p. 7290-7304.

19. Croce, C.M. and G.A. Calin, *miRNAs, cancer, and stem cell division.* Cell, 2005. **122**(1): p. 6-7.

20. Latronico, M.V., D. Catalucci, and G. Condorelli, *Emerging role of microRNAs in cardiovascular biology.* Circulation research, 2007. **101**(12): p. 1225-1236.

21. Hansen, T., et al., *Brain expressed microRNAs implicated in schizophrenia etiology.* PloS one, 2007. **2**(9): p. e873.

22. Williams, M.D. and G.M. Mitchell, *MicroRNAs in insulin resistance and obesity.* Experimental diabetes research, 2012. **2012**.

23. Akao, Y., et al., *Microvesicle-mediated RNA molecule delivery system using monocytes/macrophages.* Molecular therapy, 2011. **19**(2): p. 395-399.

24. Kusuma Jati, R., et al., *Human vascular endothelial cells transport foreign exosomes from cow's milk by endocytosis.* . Am. J. Physiol. Cell Physiol., 2016. **310**: p. C800-C807.

25. Manca, S., et al., *Milk exosomes are bioavailable and distinct microRNA cargos have unique tissue distribution patterns.* Sci. Rep., 2018. **8**(1): p. 11321.

26. Mutai, E., F. Zhou, and J. Zempleni, *Depletion of dietary bovine milk exosomes impairs sensorimotor gating and spatial learning in C57BL/6 mice.* FASEB J., 2017. **31**: p. 150.4.

27. Raposo, G. and W. Stoorvogel, *Extracellular vesicles: exosomes, microvesicles, and friends.* J. Cell Biol., 2013. **200**(4): p. 373-383.

28. Abbott, N.J., L. Rönnbäck, and E. Hansson, *Astrocyte–endothelial interactions at the blood–brain barrier.* Nature reviews neuroscience, 2006. **7**(1): p. 41.

29. Cecchelli, R., et al., *Modelling of the blood–brain barrier in drug discovery and development.* Nature reviews Drug discovery, 2007. **6**(8): p. 650.

30. Kreutzberg, G.W., *Microglia: a sensor for pathological events in the CNS.* Trends in neurosciences, 1996. **19**(8): p. 312-318.

31. Colonna, M. and O. Butovsky, *Microglia function in the central nervous system during health and neurodegeneration.* Annual review of immunology, 2017. **35**: p. 441-468.

32. Sevenich, L., *Brain-resident microglia and blood-borne macrophages orchestrate central nervous system inflammation in neurodegenerative disorders and brain cancer.* Frontiers in immunology, 2018. **9**: p. 697.

33. Pardridge, W.M., *Drug transport across the blood–brain barrier.* Journal of cerebral blood flow & metabolism, 2012. **32**(11): p. 1959-1972.

34. Kuhnline Sloan, C.D., et al., *Analytical and biological methods for probing the blood-brain barrier.* Annual Review of Analytical Chemistry, 2012. **5**: p. 505-531.

35. Ruck, T., S. Bittner, and S.G. Meuth, *Blood-brain barrier modeling: challenges and perspectives.* Neural regeneration research, 2015. **10**(6): p. 889.

36. Amato, S.P., et al., *Whole brain imaging with serial two-photon tomography.* Frontiers in neuroanatomy, 2016. **10**: p. 31.

# CHAPTER TWO

# TRANSPORT AND DISTRIBUTION OF BOVINE MILK EXOSOMES AND MIR-34A CARGO IN MURINE CEREBRAL CORTEX ENDOTHELIAL BEND.3 CELLS AND BV2 MICROGLIA

# Transport and distribution of bovine milk exosomes and miR-34a cargo in murine cerebral cortex endothelial bEnd.3 cells and BV2 microglia

*Pearl Ebea, Sonal Sukreet, Janos Zempleni**

Department of Nutrition & Health Sciences, University of Nebraska-Lincoln, Lincoln, NE 68583-0806, USA.

Keywords: blood-brain barrier, distribution, exosomes, milk, transport kinetics.

*Corresponding Author: Janos Zempleni; 316C Leverton Hall, Lincoln, NE 68583-0806, USA; +1 402.472.3270; jzempleni2@unl.edu.

Funding sources: National Institute of Food and Agriculture 2015-67017-23181 and 2016-67001-25301, National Institutes of Health 1P20GM104320, the Nebraska University President's Office, and United States Department of Agriculture Hatch Act and W-3002 and W-4002. J.Z is a consultant for PureTech Health, Inc.

Abbreviations: BBB, blood-brain barrier; bEnd.3, murine cerebral cortex endothelial cells; BME, bovine milk exosomes; BV2, murine brain microglia; C8-D1A, murine brain cerebellum astrocytes; FBS, fetal bovine serum; $K_m$, Michaelis-Menten constant; $P_c$, permeability coefficient; PFA, para-formaldehyde; TEER, transepithelial electrical resistance; $V_{max}$, maximum velocity.

**ABSTRACT**

The blood-brain barrier (BBB) poses an obstacle in the delivery of drugs to the brain. Bovine milk exosomes (BME) are explored for delivering antisense oligonucleotides to tumors, because BME are bioavailable and protect RNA cargos against degradation in the gastrointestinal tract. This study had the following objectives: 1) assess the transport kinetics of BME and their RNA cargos and secretion of RNA across the apical membrane in murine cerebral cortex endothelial bEnd.3 cells and 2) determine whether murine brain BV2 microglia have the potential to accumulate and, therefore, eliminate BME that crossed the BBB. The uptake of BME labeled with a lipophilic membrane dye followed Michaelis-Menten kinetics in bEnd.3 cells: $V_{max}$ = 0.77 ± 0.20 x $10^{11}$ BME/(10,000 cells x 45 min); $K_m$ = 1.8 ± 2.2 x $10^{11}$ BME/mL. Transport kinetics were similar in BV2 microglia compared to bEnd.3 cells. When BME were labeled with an RNA-reactive dye and uptake was analyzed by using Z-stack confocal microscopy, it was apparent that BME entered the cytoplasm of bEnd.3 cells. Studies of BME transfected with fluorophore-labeled miR-34a suggested that detectable amounts of miR-34a were transported from the apical into the basolateral compartment in dual chamber systems. We conclude that BME deserve further exploration for drug delivery across the BBB.

## INTRODUCTION

Most cells secrete exosomes (30 - 120 nm diameter), which transfer regulatory cargos such as lipids, proteins and various species of RNA from donor cells to adjacent or distant recipient cells [1, 2]. Exosomes may trigger responses in recipient cells through binding to surface receptors or by delivering regulatory cargos to the cell interior [1-3]. Once inside cells, exosomes and their cargos may be degraded in lysosomes or elicit responses such as microRNA-dependent changes in gene expression [1, 2]. Among exosome cargos, microRNAs are of particular interest because they regulate more than 60% of human genes and loss of microRNA maturation is embryonic lethal [4, 5].

Exosomes and their microRNA and protein cargos are not solely obtained from endogenous synthesis but may also be absorbed from food matrices such as bovine milk [6-8]. Encapsulation of RNA in bovine milk exosomes (BME) confers protection against degradation under harsh conditions present in the gastrointestinal tract (low pH, RNases) and a pathway to intestinal absorption by endocytosis [7, 9]. Primary accumulation sites of BME and their microRNA cargos include intestinal mucosa, liver, spleen and brain [8]. Evidence suggests that resident macrophages accumulate foreign exosomes and thereby contribute to the observed distribution patterns, e.g., Kupffer cells in the liver and microglia in brain [10, 11].

Our discovery that BME and their cargos are bioavailable have sparked an interest in using BME as a scalable vehicle for the delivery of drugs [12, 13]. BME do not elicit adverse immune reactions following oral administration to humans, rats and human peripheral blood mononuclear cells *ex vivo* ([12], E. Mutai et al. in press). Engineered exosomes have been used to deliver antisense oligonucleotides (small interfering RNA) to pancreas and inhibition of the expression of a pro-carcinogenic mutant of KRAS [14]. The delivery of drugs to the brain poses a unique

challenge because of the blood-brain barrier (BBB), which prevents many compounds, including drugs from entering the brain [15]. It is unknown whether the accumulation of BME and microRNAs reported in previous studies represent compounds in blood vessels or whether BME and cargos crossed the BBB and entered brain tissue, although evidence suggests that the latter is the case ([8], see Discussion).

The objectives of this study were to: 1) assess the transport kinetics of BME and their RNA cargos in murine cerebral cortex endothelial bEnd.3 cells, and secretion of RNA into the basolateral chamber in a co-culture model of the BBB, and 2) determine whether murine brain BV2 microglia have the potential to accumulate and, therefore, eliminate BME that crossed the BBB.

## EXPERIMENTAL SECTION

### Cell culture

Murine brain endothelial bEnd.3 cells and murine C8-D1A astrocytes were purchased from American Type Culture Collection. Murine BV2 microglia were obtained from Dr. Sanjay Maggirwar (University of Rochester Medical Center, Rochester, NY). All cells were cultured in Dulbecco's Minimal Essential Media (Hyclone) containing 10% fetal bovine serum (Atlanta Biologicals), 1% penicillin (100 IU/mL) and streptomycin (100 μg/mL) (Gibco), and 0.1% sodium pyruvate (Sigma) and were maintained in a humidified atmosphere at 37 ˚C and 5% $CO_2$. bEnd.3 cells and BV2 microglia were used from passages 24 – 30 and 15 – 25 respectively. ATCC did not provide information about passage number for C8-D1A cells; we passaged them up to 15 times in our laboratory.

**Exosome isolation and authentication**

Fat-free bovine milk was obtained from a local grocery store and exosomes were isolated from milk by ultracentrifugation (Sorvall WX Ultra 80, F37L-8 x 100 rotor; Thermo Scientific) as described previously, with minor modifications [7, 16]. Characterization was done using scanning electron microscopy (Hitachi S4700, Hitachi) and nanoparticle tracking analysis (NanoSight NS300; Malvern). Exosomes were suspended in sterile phosphate-buffered saline (PBS) and stored at -80 °C until use.

**Transport studies in bEnd.3 cells and BV2 microglia**

For transport studies, bEnd.3 cells and BV2 microglia were seeded in conditioned media, prepared by using exosome-depleted fetal bovine serum (120,000 *g*, 18 h). Seeding densities were 7.5 x $10^3$ bEnd.3 cells and 1 x $10^4$ BV2 microglia per well in 96-well polystyrene plates. Cells were allowed to reach 70 – 80% confluence prior to conducting transport studies.

BME were labeled with the lipophilic FM 4-64 membrane dye (excitation 515 nm, emission 640 nm, Molecular Probes). Eight microliters of stock solution of FM 4-64 (5.9 mmol/L) was added to 1 mL of exosome suspension and incubated at 37 ºC for 30 min, followed by ultracentrifugation at 120,000 *g* at 4 ºC for 90 min to remove excess dye. In time-course experiments, bEnd.3 cells and BV2 microglia were incubated with 6 x $10^{11}$ BME/mL at 37 °C and 5% $CO_2$ for up to 6 h. In dose-response experiments, bEnd.3 cells and BV2 microglia were incubated with 3 x $10^{11}$ to 15 x $10^{11}$ BME/mL at 37 °C and 5% $CO_2$ for 45 min. After incubation, the media supernatant was removed, and cells were washed twice with pre-warmed PBS. Controls were prepared by incubating cells with medium only, and by removing BME

immediately after addition to cultures (t = 0 h). BME uptake by cells was measured using a microplate fluorescence reader (BioTek Instruments).

**Z-stack confocal microscopy**

Z-stack confocal microscopy was used to confirm that BME entered the cell interior, and that the uptake of FM 4-64-labeled BME was not an artifact caused by the transfer of FM 4-64 to lipophilic compounds other than BME membranes [17]. Briefly, mRNA cargos in BME were labeled by using the ExoGlow-RNA$^{TM}$ EV Labeling Kit (excitation 485 nm, emission 537 nm, System Biosciences) following the manufacturer's recommendations. bEnd.3 cells and BV2 microglia were seeded at a density of 3 x $10^4$ and 4 x $10^4$ cells per well (600µL medium), respectively, in 24-well polystyrene plates. After 24 h in culture, media were replenished and 50 µL of ExoGlow-RNA$^{TM}$-labeled BME (stock, 5 x $10^{11}$ BME/mL) was added to each well and cells were incubated at 37 °C and 5% $CO_2$ for 24 h. Prior to imaging, media supernatant was removed and cells were washed twice with pre-warmed PBS, fixed with 4% paraformaldehyde (PFA) at room temperature (RT) for 15 min (Electron Microscopy Sciences) and permeabilized with 0.1% Triton X-100 (J.T. Baker; RT, 30 min) [18]. Actin filaments and nuclei were stained with Alexa Fluor 568 phalloidin (excitation 578 nm, emission 600 nm, Invitrogen) and DAPI (excitation 358 nm, emission 461 nm, Invitrogen), respectively (RT, 30 min). Images were obtained using an A1R-Ti2 confocal system (Nikon).

**Blood-brain barrier model**

The transport of BME across the BBB was assessed by using co-cultures of bEnd.3 cells and C8-D1A astrocytes. We chose this co-culture model, because astrocytes improve the barrier

properties of brain endothelial cell cultures ([19], see Results). Studies were conducted using a transwell, dual chamber system (0.4 μm pore size, 6.5 mm diameter, 24-well polystyrene plates, Costar) [7]. Astrocytes were seeded in the basolateral chamber of 24-well polystyrene plates at a density of $4 \times 10^4$ cells/well and cultured for two days to allow for adherence to plastic surfaces. bEnd.3 cells were seeded in the polyester transwell inserts at a density of $6.6 \times 10^4$ cells/insert. Cell cultures were maintained in a humidified atmosphere at 37 ˚C and 5% $CO_2$ and the basolateral medium was renewed daily. Cells were cultured in complete Dulbecco's Minimal Essential Medium supplemented with 10% fetal bovine serum, 1% penicillin (100 IU/mL), streptomycin (100 μg/mL) and 0.1% sodium pyruvate.

bEnd.3 cell monolayer integrity was assessed by measuring transepithelial electrical resistance (TEER) on a daily basis [19]. TEER was measured by using an Epithelial Voltohmmeter (EVOM) with STX2 electrodes (EMD Millipore). Resistance readings of cell-free inserts were subtracted from resistance readings of cell-containing inserts. Values are expressed as Ohm x $cm^2$($\Omega$ $cm^2$). Lucifer yellow (LY) permeability assay was carried out as previously described [20]. Permeability coefficients ($P_c$) were calculated as follows and are expressed in units of cm/s for both BME transport and LY permeability for bEnd.3 cell monolayers:

$$P_c\ [cm/s] = \frac{V_r \text{ x } C_f}{C_i \text{ x } A \text{ x } t}$$

where $P_c$ is the permeability coefficient; $V_r$ is the receiver volume in mL; $C_f$ is the final receiver concentration in the basolateral chamber in units of BME/100 μL and μM for BME and LY, respectively; Ci is the initial apical concentration in the apical chamber in units of BME/100 μL and μM for BME and LY, respectively; and A is the membrane growth area in $cm^2$ and *t* is the assay time in seconds.

Monolayer integrity was also evaluated by assessing the expression of zonula occludens-1 (ZO-1) protein [21] in post-confluent bEnd.3 cells on coverslips (VWR). Cells were fixed and permeabilized as previously described [18], blocked with LI-COR blocking buffer (LI-COR; RT, 1 h) and incubated with Alexa Fluor 488-conjugated anti-ZO-1 (excitation 490 nm, emission 525 nm, Santa Cruz Biotechnology) at RT for 1 h. Slides were counterstained by using DAPI (RT, 15 min) and images were obtained by using an A1R-Ti2 confocal microscope.

Studies of BME transport across the bEnd.3 monolayer were initiated by removing Dulbecco's Minimal Essential Medium from both inserts and basolateral chambers and washing inserts and basolateral chambers three times with pre-warmed Hank's balanced salt solution (HBSS, Gibco). Next, 100 µL HBSS containing 6 x $10^{11}$ to 24 x $10^{11}$ fluorophore-labeled BME/100 µL was added to the inserts. Fluorophore labeling was achieved by transfecting $10^{12}$ BME with 150 pmoles of 5'-IRDye-labeled miR-34a, to produce a final stock concentration of 2 x $10^{13}$ transfected BME[8]. Cells were kept at 37 ˚C and 5% $CO_2$. At timed intervals (15, 30, 45, 60 min), 100 µL of sample was collected from the basolateral chambers and transferred into a 96-well polystyrene plate for fluorescence analysis using an Odyssey imaging system (LI-COR). The buffer in the lower chamber was replenished with an equal volume of HBSS each time a sample was collected. Fluorescence readings of sample in HBSS collected at different time points were subtracted from HBSS only.

**Statistical analyses**

Homogeneity of variances was assessed by using the Brown-Forsythe test [22]. The variance of data was heterogeneous for BBB transport in dose-dependent transwell studies even after log transformation; the data were analyzed by using the Kruskal – Wallis test followed by Dunn's

multiple comparison test. Data from time-dependent transwell studies were analyzed by using repeated measures one-way ANOVA followed by Tukey's multiple comparisons test. Comparisons between two groups were analyzed by using the unpaired two-tailed t-test. Data analysis was conducted by using GraphPad Prism 6.0 (GraphPad Software). Data are reported as mean ± SEM. Differences were considered significant if $P < 0.05$.

## RESULTS

### Transport of bovine milk exosome in bEnd.3 cells and BV2 microglia

The uptake of FM 4-64-labeled BME increased linearly with time in bEnd.3 cells ($y = 3.1 \times 10^8 x + 5.6 \times 10^9$; $R^2 = 0.99$) and BV2 microglia ($y = 3.3 \times 10^8 x + 2.5 \times 10^{10}$; $R^2 = 0.86$) for the entire observation period (Figure 2.1 A,B). Subsequent transport studies were conducted for 45 minutes. The uptake of FM 4-64 labeled BME by bEnd.3 and BV2 cells exhibited saturation kinetics and was modeled using the Michaelis-Menten equation (Figure 2.1 C). In bEnd.3 cells, maximal transport rate ($V_{max}$) and Michaelis-Menten constant ($K_m$) were $0.77 \pm 0.18 \times 10^{11}$ BME/(10,000 cells x 45 min) and $1.8 \pm 2.0 \times 10^{11}$ BME/mL respectively, whereas in BV2 microglia Vmax and $K_m$ were $0.66 \pm 0.14 \times 10^{11}$ BME/(10,000 cells x 45 min) and $1.9 \pm 1.9 \times 10^{11}$ BME/mL respectively. Analysis by Z-stack confocal microscopy suggested that BME entered the interior as opposed to adhering to the surface in bEnd.3 cells (Figure 2.2 and Figure S.3) and BV2 microglia (Figure S.5). When maximal intensity projections of all focal planes for each channel were obtained, extranuclear localization of BME was apparent in bEnd.3 cells and BV2 microglia (Figure 2.3 A,B); no exosome signal was detected in BME-free controls.

**Transport of miR-34a across the blood-brain barrier**

MiR-34a transfected into BME was transported across the BBB in a bEnd.3 cell dual chamber system. When 6.0 x $10^{11}$ BME, transfected with miR-34a were added to the apical side of bEnd.3 cells in transwell inserts, the transfer of miR-34a across cell monolayers into the basolateral chamber increased with time. The transport of mass was modest: 53 ± 4.2 arbitrary units of fluorescence at baseline (background) vs 83 ± 5.9 arbitrary units of fluorescence at t = 60 min ($P < 0.05$; Figure 2.4A). Pc values suggested that the permeability of monolayers was similar for each time point measured in the study ($P > 0.05$; Figure 2.4B). When increasing numbers of BME were added to the apical chamber, the Pc values of miR-34a transport across the BBB decreased, suggesting a saturable transport across the endothelial monolayer (Figure 2.4C). bEnd.3 cell monolayers on inserts were characterized using daily TEER measurements, LY permeability measurements and ZO-1 tight junction expression. Daily TEER measurements showed a steady increase until days 4 - 5 post seeding when readings reached a plateau (Figure 2.5A). Endothelial cell monoculture showed significantly lower TEER values (~24 Ω x $cm^2$) compared to endothelial cell/astrocyte co-cultures (~34 Ω x $cm^2$); in monocultures TEER values peaked on day 3. Subsequent permeability studies were carried out in co-cultures and data were measured on day 5. These data are consistent with previous reports suggesting that the presence of astrocytes enhances the formation of tight bEnd.3 cell monolayers[19]. bEnd.3 monolayers using antibody to ZO-1 protein revealed tight junctions expressed ZO-1, which is a marker for the formation of tight junctions [23] (Figure 2.5B). $P_c$ values were ~ 6.7 x $10^{-6}$ cm/s in LY permeability assays, which is similar to previous studies of BBB in endothelial cells from rat and bovine origin[21].

**DISCUSSION**

This paper is first to show that brain endothelial cells take up BME administered. In a previous paper we reported that milk exosomes and select protein and microRNA cargos accumulate in the brain in pigs and mice, but we did not assess whether the exosomes were in the blood vessels or delivered to brain cells[8]. This paper advanced the existing knowledge base by demonstrating that BME enter the cytoplasm in murine brain endothelial cells and are subsequently transferred across the basolateral membrane, which are the two key events in the transport of compounds across the BBB[23]. Our observation that BME cross the BBB barrier is consistent with a previous study, which suggested that exosomes from the human glioblastoma cell line, LN18 delivered cre recombinase to the brain in Ai14 reporter mice, eliciting a switch from the expression of green fluorescent protein to the expression of tdTomato in cerebellum, cortex, hippocampus, olfactory bulb and striatum[24]. The study also suggest that exosomes transfer cargos in quantities sufficient to elicit biological effects, in that case cre recombination. While the transfer of miR-34a cargo across a bEnd.3 cell monolayer was quantitatively moderate (approximately two times background), the depletion of BME was sufficient to elicit a significant loss in spatial learning and memory in preliminary studies in mice fed BME and RNA-depleted diets[25]. Note that small changes in microRNA abundance may alter gene expression, with the effect size depending on the pool of mRNA transcripts targets in a given cell or tissue [26]. Also, distinct microRNA cargos in BME have unique distribution patterns and it is conceivable that microRNAs other than miR-34a accumulate in comparably large quantities in brain[8]. The distribution of BME in bEnd.3 cells and BV2 microglia reported in this paper is consistent with expectations: BME accumulated in the extranuclear space, presumably in endosomes, multivesicular bodies and lysosomes[1, 2].

One of the strengths of this study is that the data reported here are not fraught with the uncertainty whether a (lipophilic) dye dissociated from the BME membrane and whether BME entered cells as opposed to adhere to the cell surface. Lipophilic dyes such as DiR and PKH67 may detach from membranes and transfer to lipoproteins and proteins, thereby causing artifacts in studies of exosome transport, bioavailability and distribution[17]. We formally excluded these possibilities by transfecting BME with miR-34a covalently conjugated with a fluorophore, and by confirming uptake into the cell interior by Z-stack confocal microscopy. In previous studies, we used fluorophore-quencher co-labeling to confirm that microRNA-fluorophore conjugates are stable when administered to mice[8]. Therefore, signals observed in BME are unlikely due to artifacts caused by the transfer of dye to lipophilic compounds other than BME membranes. This being said, the mere binding of exosomes to cell surfaces may also elicit cellular responses such as activation of p38 and pERK signaling[3].

Our studies suggest that the capacity and affinity for BME transport are similar in brain endothelial cells and macrophages (microglia). This is an important observation, because previous studies suggest that foreign exosomes are rapidly eliminated by macrophages[11]. Rapid elimination of BME by macrophages could reduce the biological activity of BME in both nutrition and drug delivery. Studies of bEnd.3 and BV2 cultures do not formally exclude the possibility that BME might be eliminated by macrophages in tissues other than brain in a whole organism. Future studies will need to determine whether BME transport across the BBB barrier is a selective process that discriminates against some sub-populations of BME.

In conclusion, this study demonstrated that BME are taken up by the brain which is consistent with effects reported for dietary BME and brain function, and the use of BME for delivering antisense-based cancer drugs across the BBB. Future studies will need to identify

factors that permit directing BME to target sites, e.g., tumors and determine whether the uptake of BME by cancerous cells exceeds that of non-cancerous cells.

**Acknowledgment**

The authors acknowledge the use of the Biomedical and Obesity Research Core and the assistance of Dr. Steven Kachman in the Nebraska Center for the Prevention of Obesity Disease through Dietary Molecules at the University of Nebraska-Lincoln. The authors also acknowledge Terri Fangman for assistance with acquisition of confocal microscopy images and Dr. Moreau's lab for assistance with the use of their Epithelial Voltohmmeter (EVOM).

**REFERENCES**

1. Yanez-Mo, M.; Siljander, P. R.; Andreu, Z.; Zavec, A. B.; Borras, F. E.; Buzas, E. I.; Buzas, K.; Casal, E.; Cappello, F.; Carvalho, J.; Colas, E.; Cordeiro-da Silva, A.; Fais, S.; Falcon-Perez, J. M.; Ghobrial, I. M.; Giebel, B.; Gimona, M.; Graner, M.; Gursel, I.; Gursel, M.; Heegaard, N. H.; Hendrix, A.; Kierulf, P.; Kokubun, K.; Kosanovic, M.; Kralj-Iglic, V.; Kramer-Albers, E. M.; Laitinen, S.; Lasser, C.; Lener, T.; Ligeti, E.; Line, A.; Lipps, G.; Llorente, A.; Lotvall, J.; Mancek-Keber, M.; Marcilla, A.; Mittelbrunn, M.; Nazarenko, I.; Nolte-'t Hoen, E. N.; Nyman, T. A.; O'Driscoll, L.; Olivan, M.; Oliveira, C.; Pallinger, E.; Del Portillo, H. A.; Reventos, J.; Rigau, M.; Rohde, E.; Sammar, M.; Sanchez-Madrid, F.; Santarem, N.; Schallmoser, K.; Ostenfeld, M. S.; Stoorvogel, W.; Stukelj, R.; Van der Grein, S. G.; Vasconcelos, M. H.; Wauben, M. H.; De Wever, O., Biological properties of extracellular vesicles and their physiological functions. *J. Extracell. Vesicles* **2015,** *4*, 27066.

2. Abels, E. R.; Breakefield, X. O., Introduction to Extracellular Vesicles: Biogenesis, RNA Cargo Selection, Content, Release, and Uptake. *Cell. Mol. Neurobiol.* **2016,** *36*, 301.

3. Purushothaman, A.; Bandari, S. K.; Liu, J.; Mobley, J. A.; Brown, E. E.; Sanderson, R. D., Fibronectin on the Surface of Myeloma Cell-derived Exosomes Mediates Exosome-Cell Interactions. *J. Biol. Chem.* **2016,** *291* (4), 1652-1663.

4. Friedman, R. C.; Farh, K. K.; Burge, C. B.; Bartel, D. P., Most mammalian mRNAs are conserved targets of microRNAs. *Genome Res.* **2009,** *19* (1), 92-105.

5. Bernstein, E.; Kim, S. Y.; Carmell, M. A.; Murchison, E. P.; Alcorn, H.; Li, M. Z.; Mills, A. A.; Elledge, S. J.; Anderson, K. V.; Hannon, G. J., Dicer is essential for mouse development. *Nat. Genet.* **2003,** *35* (3), 215-217.

6. Baier, S. R.; Nguyen, C.; Xie, F.; Wood, J. R.; Zempleni, J., MicroRNAs are absorbed in biologically meaningful amounts from nutritionally relevant doses of cow's milk and affect gene expression in peripheral blood mononuclear cells, HEK-293 kidney cell cultures, and mouse livers. *J. Nutr.* **2014,** *144*, 1495-1500.

7. Wolf, T.; Baier, S. R.; Zempleni, J., The intestinal transport of bovine milk exosomes is mediated by endocytosis in human colon carcinoma caco-2 cells and rat small intestinal IEC-6 cells. *J. Nutr.* **2015,** *145*, 2201-2206.

8. Manca, S.; Upadhyaya, B.; Mutai, E.; Desaulniers, A. T.; Cederberg, R. A.; White, B. R.; Zempleni, J., Milk exosomes are bioavailable and distinct microRNA cargos have unique tissue distribution patterns. *Sci. Rep.* **2018,** *8* (1), 11321.

9. Izumi, H.; Kosaka, N.; Shimizu, T.; Sekine, K.; Ochiya, T.; Takase, M., Bovine milk contains microRNA and messenger RNA that are stable under degradative conditions. *J. Dairy Sci.* **2012,** *95* (9), 4831-4841.

10. Wiklander, O. P.; Nordin, J. Z.; O'Loughlin, A.; Gustafsson, Y.; Corso, G.; Mager, I.; Vader, P.; Lee, Y.; Sork, H.; Seow, Y.; Heldring, N.; Alvarez-Erviti, L.; Smith, C. E.; Le Blanc, K.; Macchiarini, P.; Jungebluth, P.; Wood, M. J.; Andaloussi, S. E., Extracellular vesicle in vivo biodistribution is determined by cell source, route of administration and targeting. *J. Extracell. Vesicles* **2015,** *4*, 26316.

11. Imai, T.; Takahashi, Y.; Nishikawa, M.; Kato, K.; Morishita, M.; Yamashita, T.; Matsumoto, A.; Charoenviriyakul, C.; Takakura, Y., Macrophage-dependent clearance of systemically administered B16BL6-derived exosomes from the blood circulation in mice. *J. Extracell. Vesicles* **2015,** *4*, 26238.

12. Munagala, R.; Aqil, F.; Jeyabalan, J.; Gupta, R. C., Bovine milk-derived exosomes for drug delivery. *Cancer Lett.* **2016,** *371* (1), 48-61.

13. Agrawal, A. K.; Aqil, F.; Jeyabalan, J.; Spencer, W. A.; Beck, J.; Gachuki, B. W.; Alhakeem, S. S.; Oben, K.; Munagala, R.; Bondada, S.; Gupta, R. C., Milk-derived exosomes for oral delivery of paclitaxel. *Nanomedicine* **2017,** *13* (5), 1627-1636.

14. Kamerkar, S.; LeBleu, V. S.; Sugimoto, H.; Yang, S.; Ruivo, C. F.; Melo, S. A.; Lee, J. J.; Kalluri, R., Exosomes facilitate therapeutic targeting of oncogenic KRAS in pancreatic cancer. *Nature* **2017,** *546* (7659), 498.

15. Pardridge, W. M., Drug transport across the blood–brain barrier. *Journal of cerebral blood flow & metabolism* **2012,** *32* (11), 1959-1972.

16. Izumi, H.; Tsuda, M.; Sato, Y.; Kosaka, N.; Ochiya, T.; Iwamoto, H.; Namba, K.; Takeda, Y., Bovine milk exosomes contain microRNA and mRNA and are taken up by human macrophages. *J. Dairy Sci.* **2015,** *98* (5), 2920-2933.

17. Takov, K.; Yellon, D. M.; Davidson, S. M., Confounding factors in vesicle uptake studies using fluorescent lipophilic membrane dyes. *J. Extracell. Vesicles* **2017,** *6* (1), 1388731.

18. Wuest, D. M.; Wing, A. M.; Lee, K. H., Membrane configuration optimization for a murine in vitro blood–brain barrier model. *Journal of neuroscience methods* **2013,** *212* (2), 211-221.

19. Wuest, D. M.; Lee, K. H., Optimization of endothelial cell growth in a murine in vitro blood–brain barrier model. *Biotechnology journal* **2012,** *7* (3), 409-417.

20. Corning, I. Corning HTS Transwell-96 Permeable Support Protocols for Drug Transport. http://www.level.com.tw/html/ezcatfiles/vipweb20/img/img/34961/2-10t_HTS_Transwell_96_Protocols_Drug_Transport_CLS-AN-058.pdf (accessed 12/15/2013).

21. Helms, H. C.; Abbott, N. J.; Burek, M.; Cecchelli, R.; Couraud, P.-O.; Deli, M. A.; Förster, C.; Galla, H. J.; Romero, I. A.; Shusta, E. V., In vitro models of the blood–brain barrier: an overview of commonly used brain endothelial cell culture models and guidelines for their use. *Journal of Cerebral Blood Flow & Metabolism* **2016,** *36* (5), 862-890.

22. Howell, D. C., *Statistical methods for psychology*. Wadsworth Cengage Learning: [Belmont, Calif?], 2013.

23. Abbott, N. J.; Rönnbäck, L.; Hansson, E., Astrocyte–endothelial interactions at the blood–brain barrier. *Nature reviews neuroscience* **2006,** *7* (1), 41.

24. Sterzenbach, U.; Putz, U.; Low, L. H.; Silke, J.; Tan, S. S.; Howitt, J., Engineered exosomes as vehicles for biologically active proteins. *Mol. Ther.* **2017,** *25*, 1269-1278.

25. Mutai, E.; Zhou, F.; Zempleni, J., Depletion of dietary bovine milk exosomes impairs sensorimotor gating and spatial learning in C57BL/6 mice. *FASEB J.* **2017,** *31*, 150.4.

26. Arvey, A.; Larsson, E.; Sander, C.; Leslie, C. S.; Marks, D. S., Target mRNA abundance dilutes microRNA and siRNA activity. *Molecular systems biology* **2010,** *6* (1).

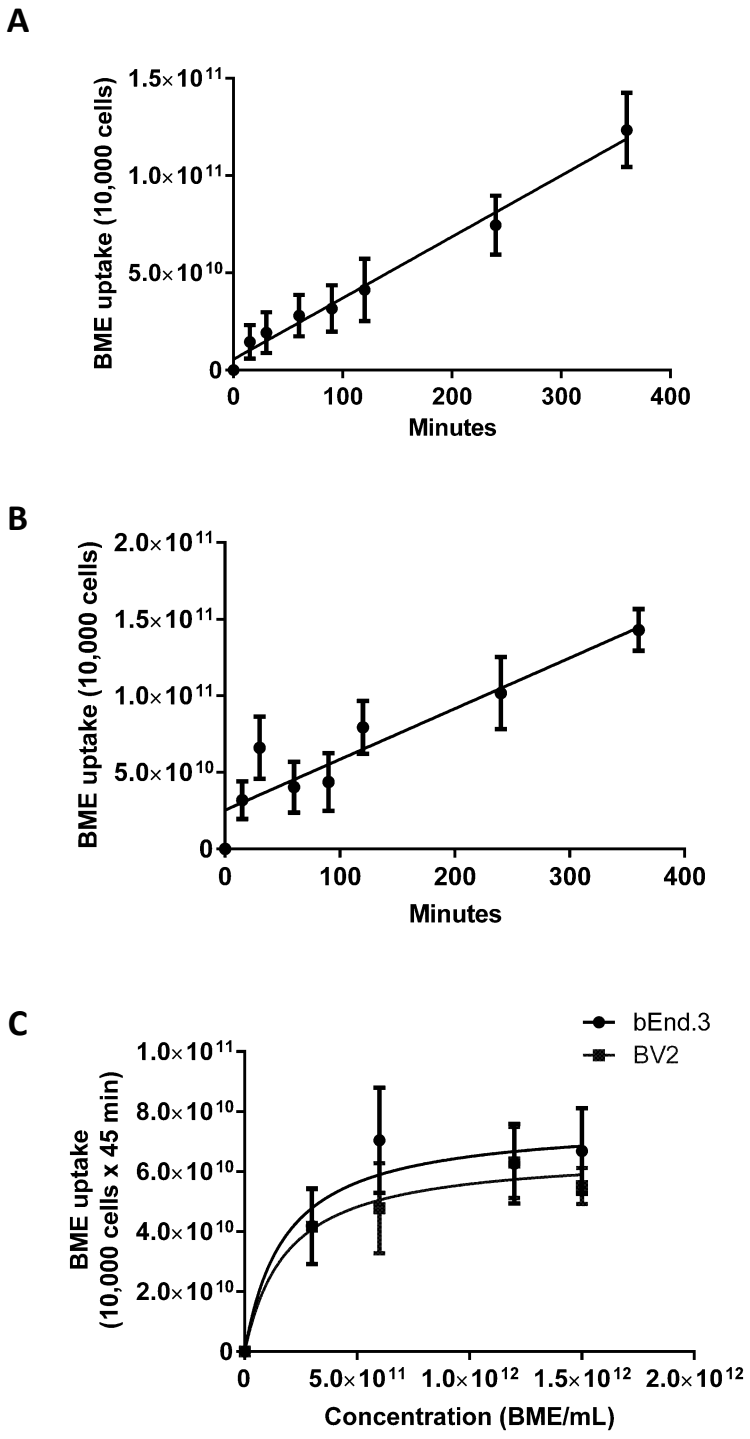


Figure 2. 1 The uptake of bovine milk exosomes (BME) by brain endothelial bEnd.3 cells and BV2 microglia increases linearly with time and is a saturable process. Time courses of BME

uptake by bEnd.3 cells (A) and BV2 microglia (B) for a concentration of 6 x $10^{11}$ BME/mL media (n = 3 biological repeats). Dose-response curves of BME uptake by bEnd.3 cells and BV2 microglia for an incubation time of 45 min, n = 3 biological repeats (C). Data are presented as mean ± SEM.

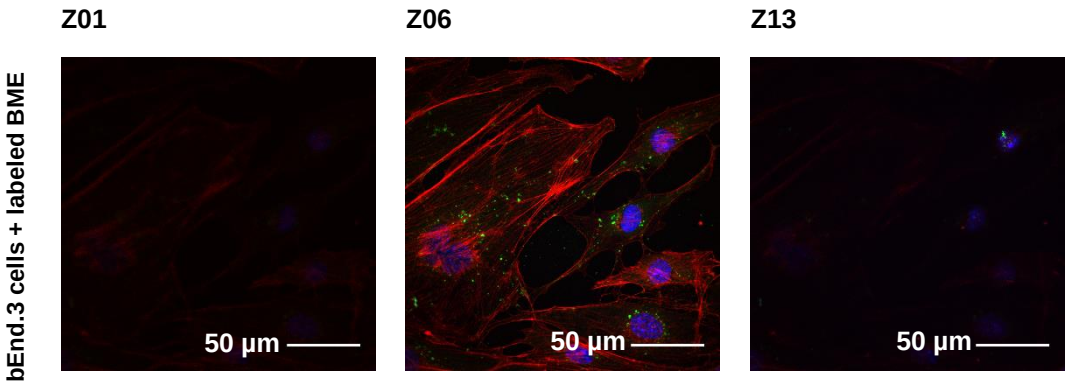


Figure 2. 2 BME enter the interior of bEnd.3 cells. Images represent select focal planes acquired by Z-stack confocal microscopy; see Figure S.3 for a complete set of planes that were acquired. mRNA in BME was labeled with ExoGlow-RNA$^{TM}$ (green). Nuclei and actin (cytoplasm) were stained with DAPI (blue) and Alexa Fluor 568 phalloidin (red), respectively. Merged images are shown. Magnification = 60x.

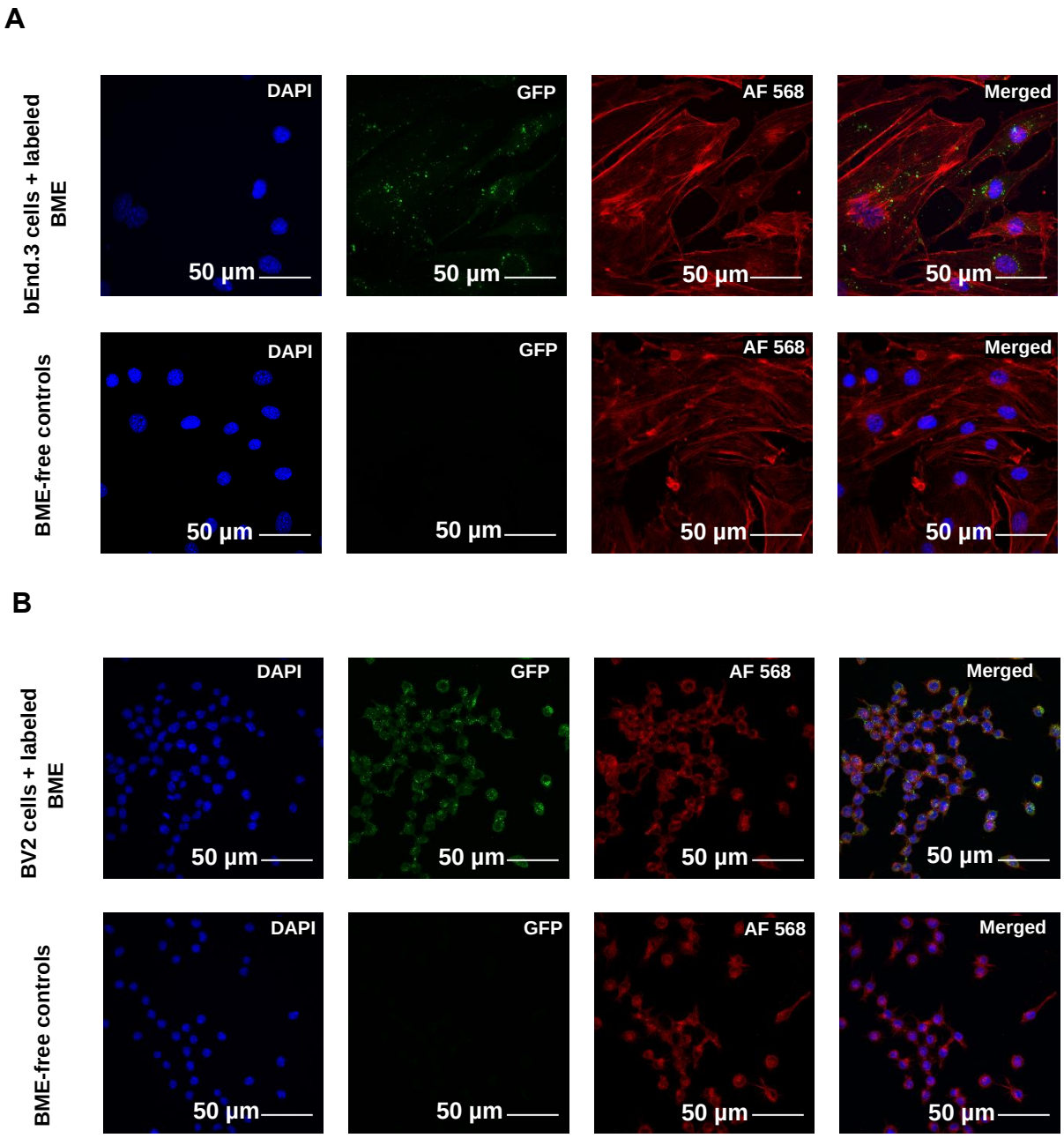


Figure 2. 3 BME localize to the extranuclear space in endothelial bEnd.3 cells and BV2 microglia. Cells were incubated for 24 h with BME in which mRNA was labeled with ExoGlow-RNA$^{TM}$ (green); controls were cells only. Nuclei and actin (cytoplasm) were stained with DAPI (blue) and Alexa Fluor 568 phalloidin (red) respectively and assessed by Z-stack confocal

microscopy (see Figures S.3 – S.6) in bEnd.3 cells (A) and BV2 cells (B). Magnification = 60x.

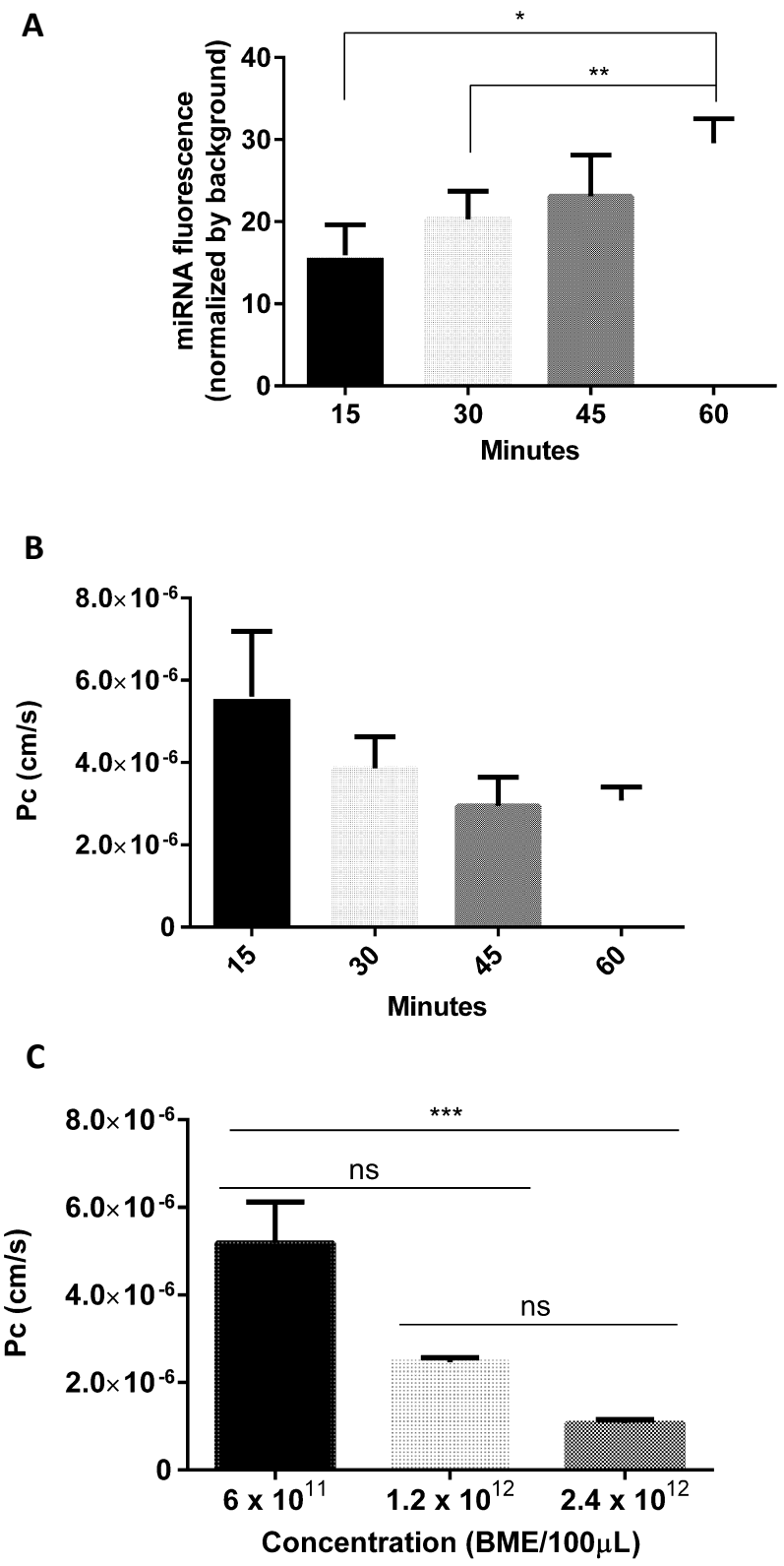

Figure 2. 4 MiR-34a-loaded BME are transported across bEnd.3 cell monolayers. (A) Transport of miR-34a transfected exosomes across an in vitro BBB model increased with time. (B) Monolayers also showed similar permeability to BME at different time points, when bEnd.3 cell monolayers were administered 6.0 x $10^{11}$ BME transfected with miR-34a (n = 3 biological repeats). (C) When cells were administered increasing concentrations of BME: 6, 12 or 24 x $10^{11}$, a decrease in permeability coefficient values was observed when measured at t = 1 h (n = 3 biological repeats measured twice each). Data are presented as mean ± SEM.

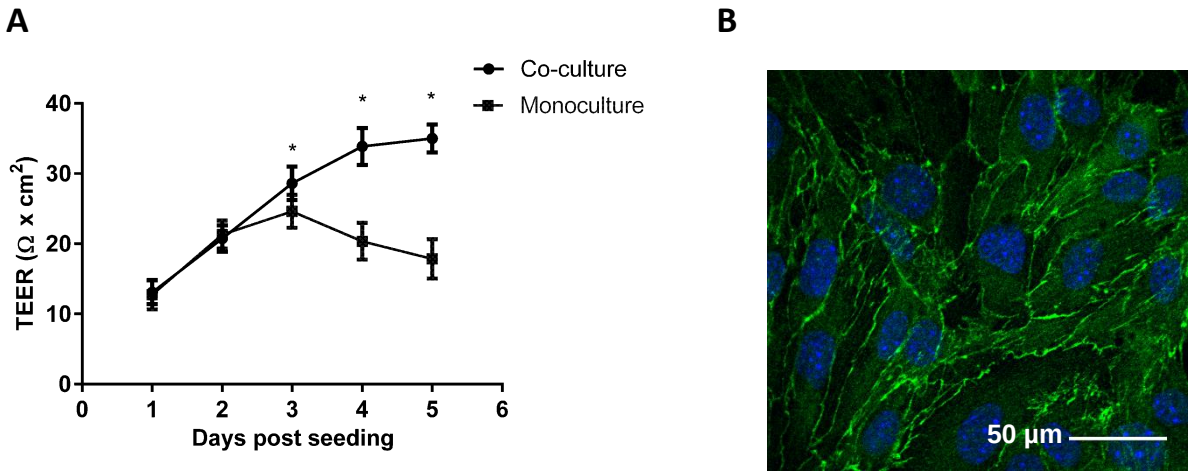


Figure 2. 5 bEnd.3 cell cultures formed a tight monolayer. (A) Comparison of electrical resistance (TEER) in bEnd.3 cell monocultures and bEnd.3 cells co-cultured with astrocytes. TEER values reached a plateau at t = 4-5 days post seeding in bEnd.3 cells co-cultures (n = 3 biological repeats, means ± SEM). *Significantly different compared to bEnd.3 cell monocultures ($P < 0.05$). (B) Immunostaining of ZO-1 in endothelial bEnd.3 monolayers. Cells were stained with anti-ZO1-conjugated Alexa Fluor 488 (green) and counterstained with DAPI (blue). Magnification = 60x; scale bar = 50 µm.

**A**

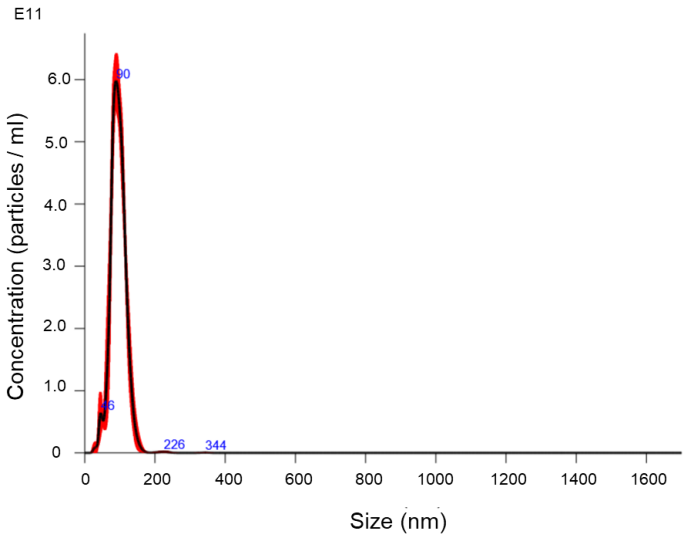


**B**

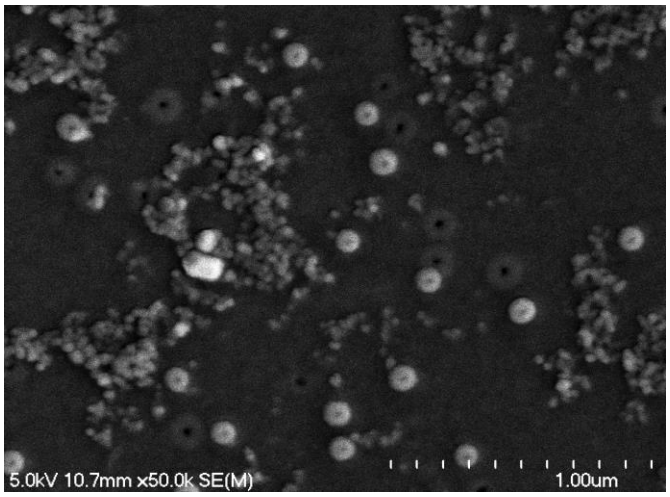


Figure S. 1 BME authentication was conducted using nanoparticle tracking analysis (A) and transmission electron microscopy (B).

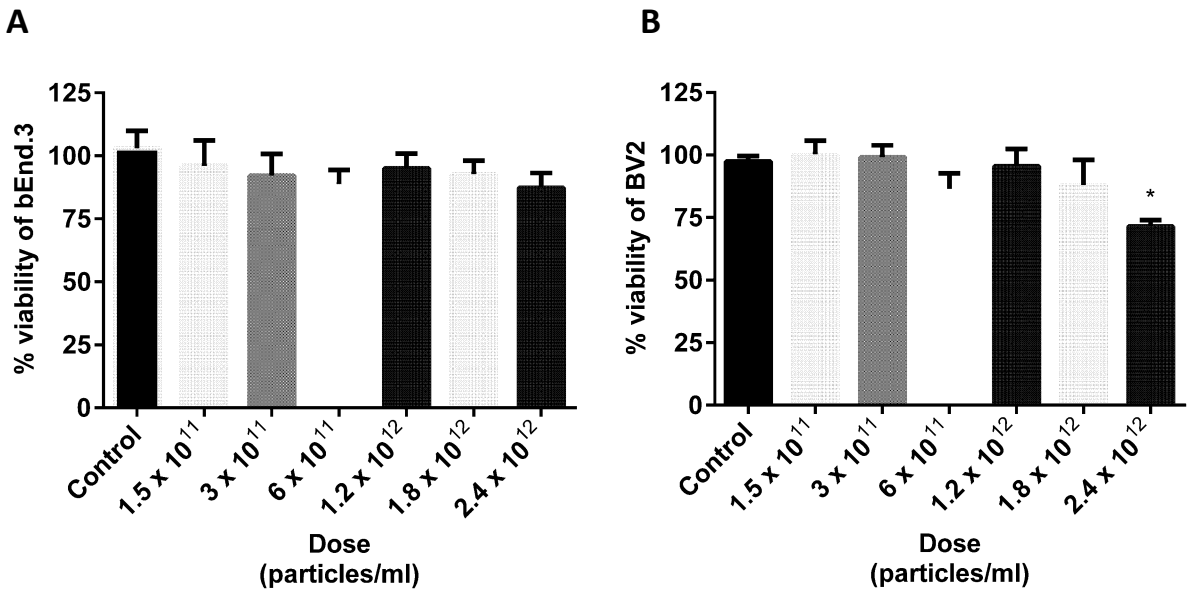


Figure S. 2 Effect of BME on cell viability. bEnd.3 cells (A) and BV2 microglia (B) were administered FM 4-64 labeled BME at concentrations similar to those used in FM 4-64 transport assays ($1.5 \times 10^{11} – 24 \times 10^{11}$ BME/mL) and monitored for 45 min. Viability was assessed using the thiazolyl blue tetrazolium bromide reagent. Data are presented as mean ± SEM (n = 3). Statistical significance was assessed by one-way ANOVA. *, $P < 0.05$ when data were compared with BME-free control cells.

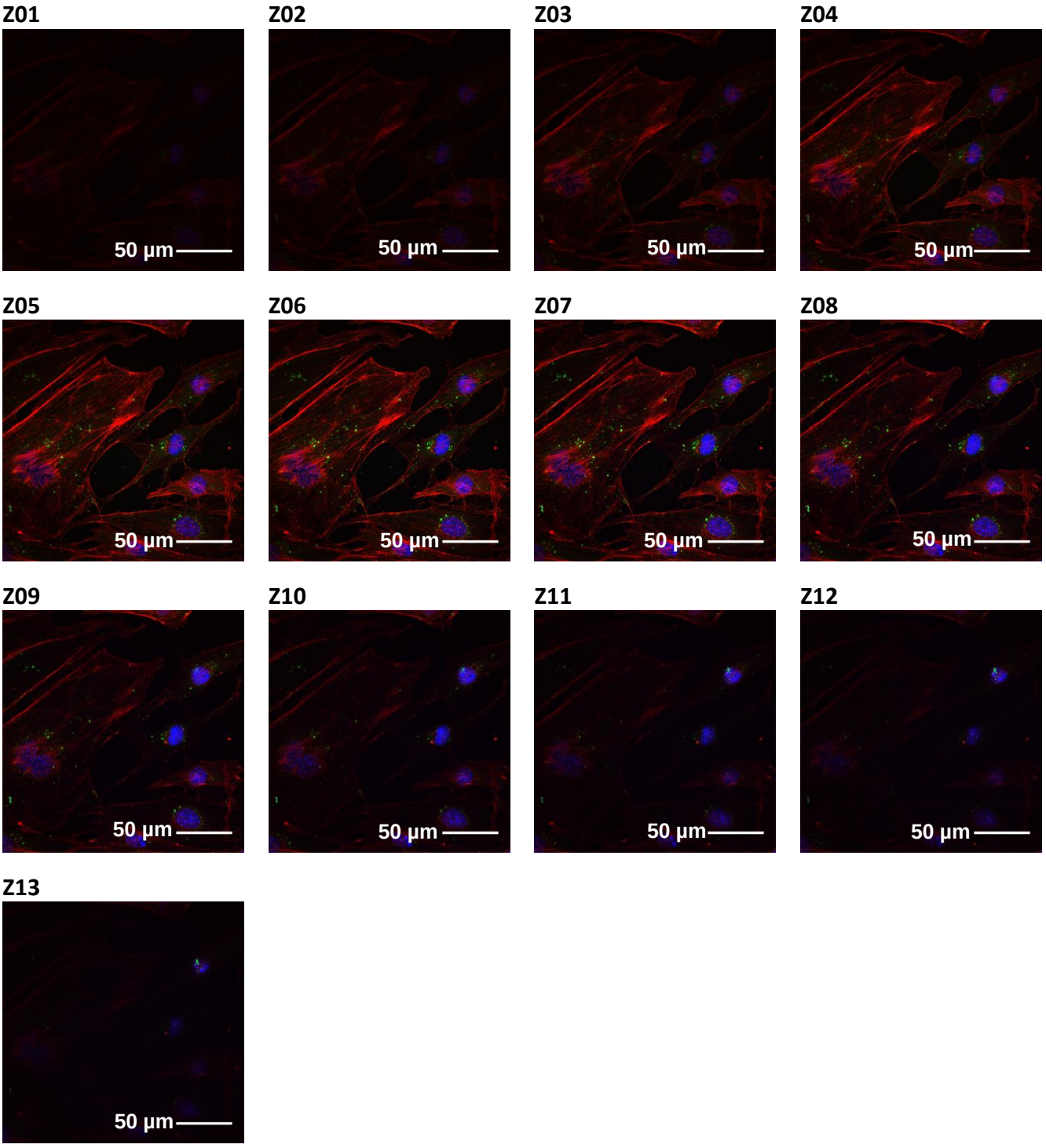
Z01
50 µm
Z02
50 µm
Z03
50 µm
Z04
50 µm
Z05
50 µm
Z06
50 µm
Z07
50 µm
Z08
50 µm
Z09
50 µm
Z10
50 µm
Z11
50 µm
Z12
50 µm
Z13
50 µm

Figure S. 3 Overlay of individual Z-stack slices for bEnd.3 cells treatment group. Cells were incubated with BME in which mRNA was labeled with ExoGlow-RNA™ (green) for 24 h. Nuclei and actin (cytoplasm) were stained with DAPI (blue) and Alexa Fluor 568 phalloidin (red) respectively. Magnification = 60x; scale bar = 50μm.

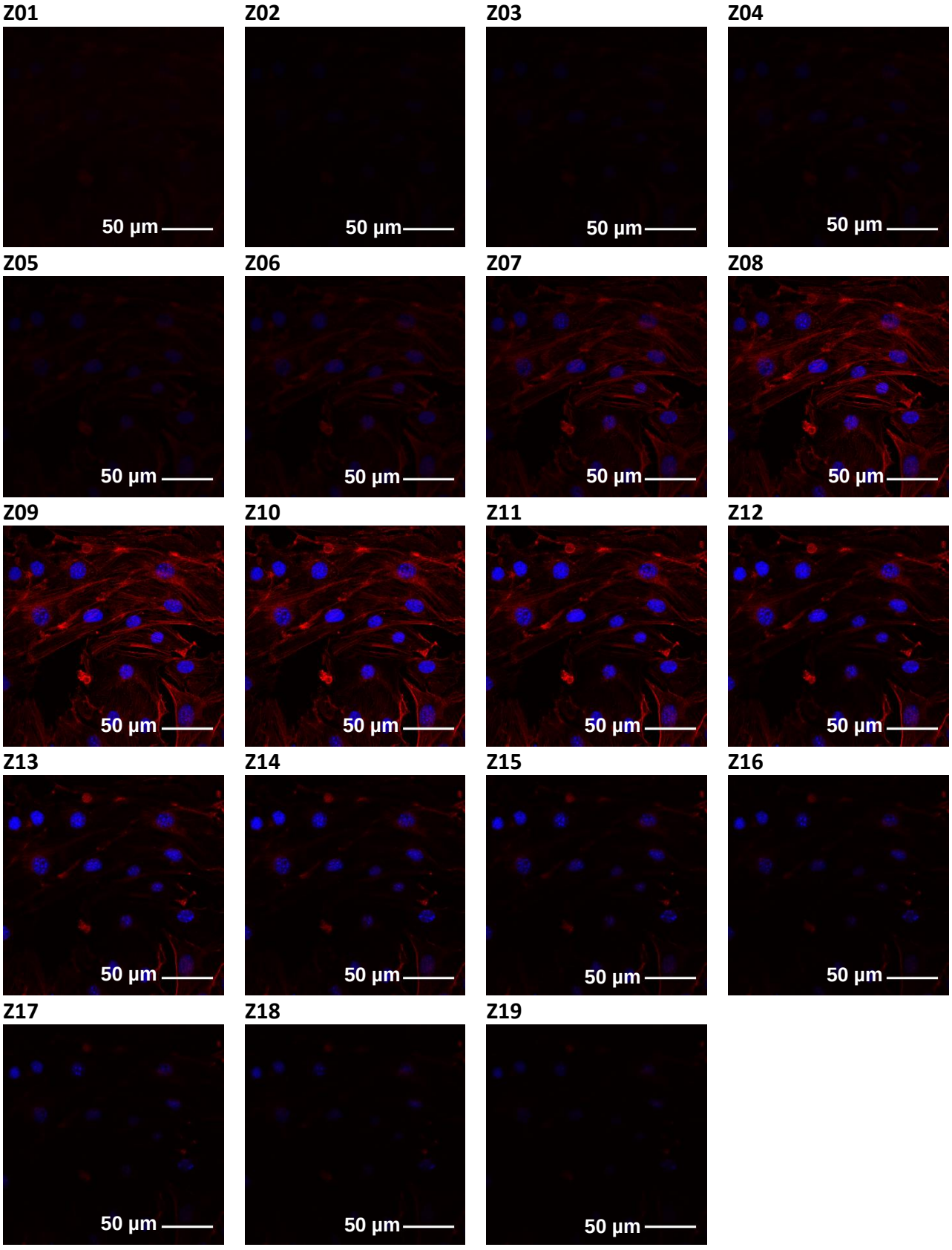
Z01
50 µm
Z02
50 µm
Z03
50 µm
Z04
50 µm
Z05
50 µm
Z06
50 µm
Z07
50 µm
Z08
50 µm
Z09
50 µm
Z10
50 µm
Z11
50 µm
Z12
50 µm
Z13
50 µm
Z14
50 µm
Z15
50 µm
Z16
50 µm
Z17
50 µm
Z18
50 µm
Z19
50 µm

Figure S. 4 Overlay of individual Z-stack slices for bEnd.3 cells control group (cells only). Nuclei and actin (cytoplasm) were stained with DAPI (blue) and Alexa Fluor 568 phalloidin (red) respectively. Magnification = 60x; scale bar = 50µm.

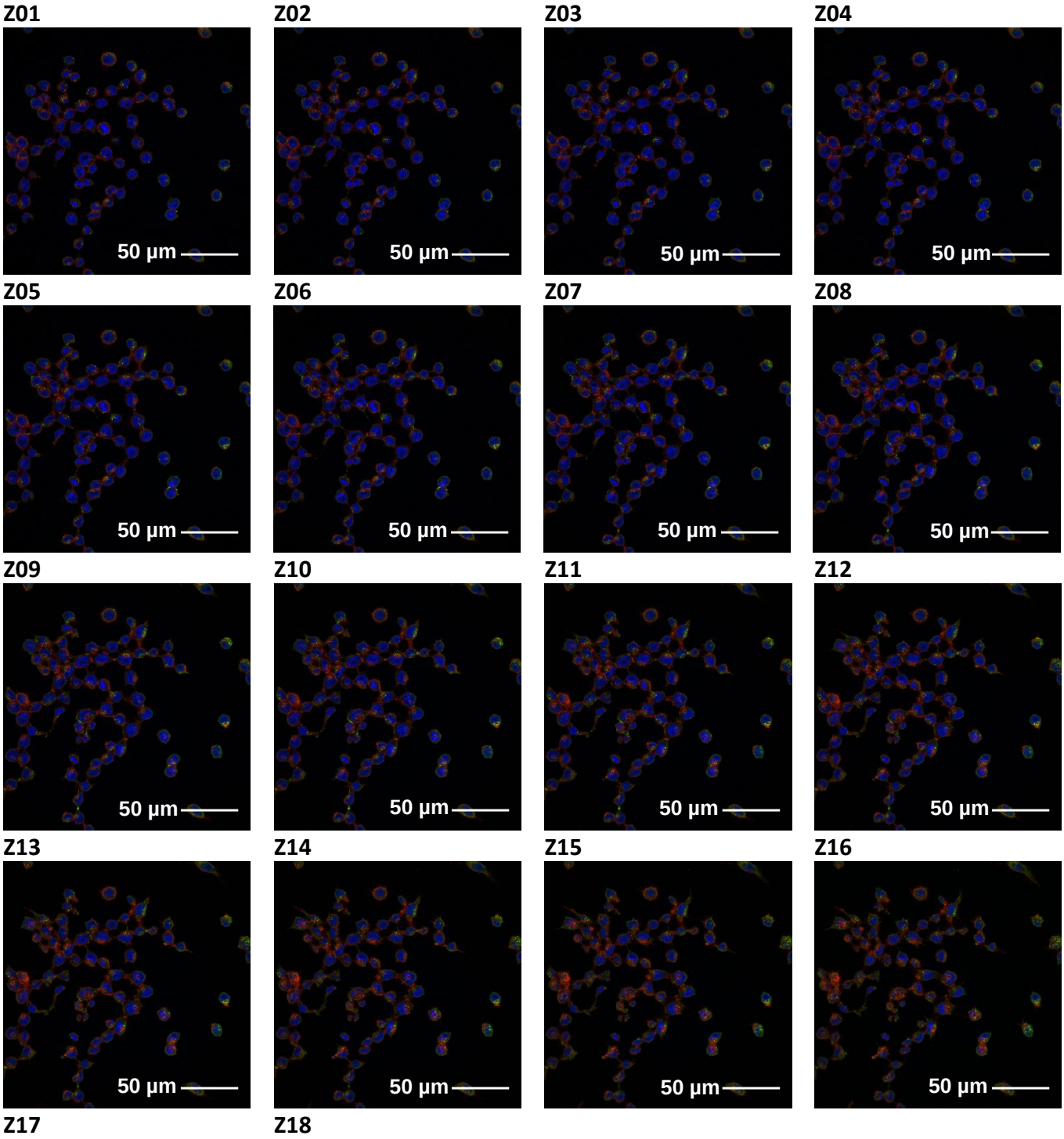
Z01
Z02
Z03
Z04
Z05
Z06
Z07
Z08
Z09
Z10
Z11
Z12
Z13
Z14
Z15
Z16
Z17
Z18
50 µm

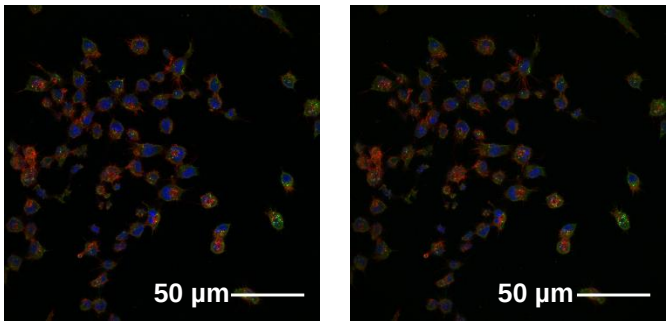


Figure S. 5 Overlay of individual Z-stack slices for BV2 cells treatment group. Cells were incubated with BME in which mRNA was labeled with ExoGlow-RNA$^{TM}$ (green) for 24 h. Nuclei and actin (cytoplasm) were stained with DAPI (blue) and Alexa Fluor 568 phalloidin (red) respectively. Magnification = 60x; scale bar = 50µm.

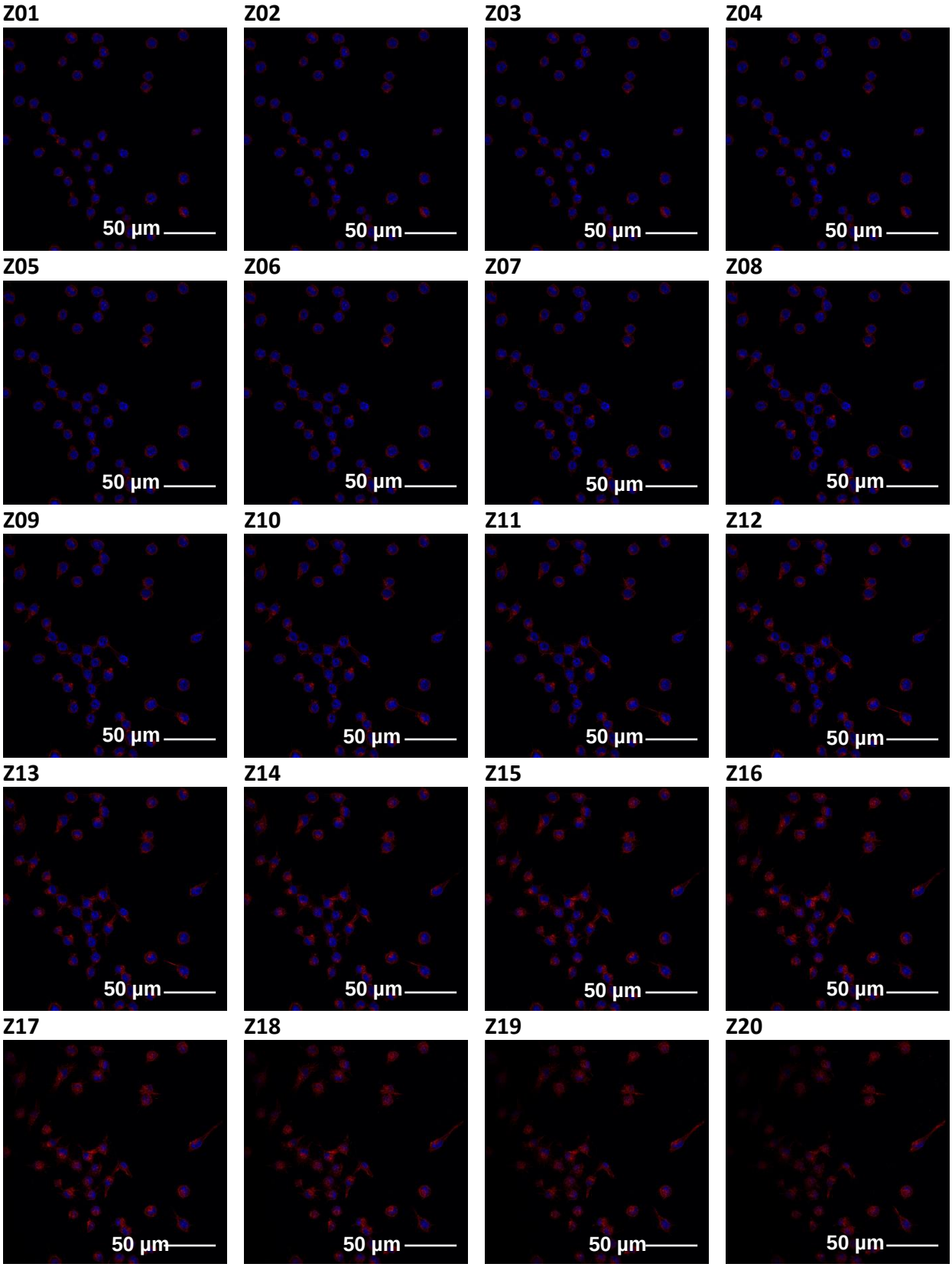
Z01
Z02
Z03
Z04
Z05
Z06
Z07
Z08
Z09
Z10
Z11
Z12
Z13
Z14
Z15
Z16
Z17
Z18
Z19
Z20
50 µm

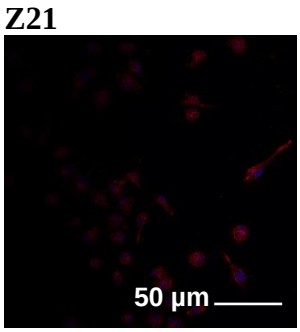


Figure S. 6 Overlay of individual Z-stack slices for BV2 cells control group (cells only). Nuclei and actin (cytoplasm) were stained with DAPI (blue) and Alexa Fluor 568 phalloidin (red) respectively. Magnification = 60x; scale bar = 50µm.

# FUTURE STUDIES

## FUTURE STUDIES

Till date, findings from our research group and others have shown that BME hold much promise as therapeutic drug delivery or biomolecule delivery vehicles due to their size, biocompatibility, safety and cost-effectiveness making them advantageous over synthetic nanoparticle formulations [1-4]. However, further research will be required to advance their therapeutic potential.

In this study, we have shown the ability of brain endothelial cells to take up BME and RNA cargos and their transport across the BBB, which supports findings by Manca and colleagues on accumulation of exosome cargos in the brain [3]. To further these results, ongoing studies are looking into the biodistribution patterns of exosome cargos in the brain. In line with this report [3] which revealed the accumulation of miR-34a transfected exosomes and endogenous CD63/eGFP-labeled exosomes in the brain of wild-type mouse pups nursed by CD63/eGFP-positive dams, ongoing experiments will examine what brain regions and cell types such as neurons or microglia may accumulate these exosomes. Knowledge of the localization of these exosomes could provide more insight into optimal delivery conditions in order to ensure maximum efficacy of therapeutically-delivered exosomes to the brain.

Also, some studies in our lab have shown that glycoproteins on the surface of exosomes are important in exosome recognition by the recipient cell and their modifications were particularly important for the uptake of bovine milk exosomes by Caco-2 and FHs cells [5]. With relation to the brain, it will be interesting to see how these glycoprotein modifications may influence the targeting and delivery of BME and RNA cargos to different tissues particularly the brain, this area is being explored in ongoing studies in our lab.

In addition, research in our lab discovered that exosome and RNA supplementation or depletion from the diet of mice produces effects on the spatial learning and memory in mice [6]. This is an interesting finding and an understanding of the mechanisms behind it will be beneficial. Previous reports have linked spatial and recognition memory with the hippocampal region of the brain [7]. As such, current and future experiments are looking into examining if any observed difference may exist between hippocampal neurons in mice fed exosome sufficient and exosome depleted diet, which may, to some extent, explain the observed differences in spatial learning and memory. Information from these studies will contribute significantly to the application of BME as a potential therapeutic delivery system and the importance of BME in brain function.

**REFERENCES**


1. Agrawal, A.K., et al., *Milk-derived exosomes for oral delivery of paclitaxel.* Nanomedicine, 2017. **13**(5): p. 1627-1636.
2. Baier, S.R., et al., *MicroRNAs are absorbed in biologically meaningful amounts from nutritionally relevant doses of cow's milk and affect gene expression in peripheral blood mononuclear cells, HEK-293 kidney cell cultures, and mouse livers.* J. Nutr., 2014. **144**: p. 1495-1500.
3. Manca, S., et al., *Milk exosomes are bioavailable and distinct microRNA cargos have unique tissue distribution patterns.* Sci. Rep., 2018. **8**(1): p. 11321.
4. Munagala, R., et al., *Bovine milk-derived exosomes for drug delivery.* Cancer Lett., 2016. **371**(1): p. 48-61.
5. Zempleni, J., et al., *Milk-derived exosomes and metabolic regulation.* Annual review of animal biosciences, 2019. **7**: p. 245-262.
6. Mutai, E., F. Zhou, and J. Zempleni, *Depletion of dietary bovine milk exosomes impairs sensorimotor gating and spatial learning in C57BL/6 mice.* FASEB J., 2017. **31**: p. 150.4.
7. Broadbent, N.J., L.R. Squire, and R.E. Clark, *Spatial memory, recognition memory, and the hippocampus.* Proceedings of the National Academy of Sciences, 2004. **101**(40): p. 14515-14520.

# APPENDIX

**Table 1.** Dose - response data for bEnd.3 transport study with FM 4-64 labeled BME.

| Concentration (BME/mL) | Uptake fluorescence (10,000 cells x 45 min) | | | | | | | | | Mean | SEM |
|---|---|---|---|---|---|---|---|---|---|---|---|
| 0.0E+00 | 0.0E+00 | 0.0E+00 | 0.0E+00 | 0.0E+00 | 0.0E+00 | 0.0E+00 | 0.0E+00 | 0.0E+00 | 0.0E+00 | 0.0E+00 | 0.0E+00 |
| 3.0E+11 | 2.8E+10 | 2.1E+10 | 0.0E+00 | 6.1E+10 | 8.7E+10 | 1.1E+10 | 1.0E+11 | 4.2E+09 | 6.1E+10 | 4.2E+10 | 1.3E+10 |
| 6.0E+11 | 7.2E+10 | 7.2E+10 | 1.1E+11 | 1.4E+11 | 7.4E+10 | 3.2E+10 | 1.4E+11 | 0.0E+00 | 0.0E+00 | 7.0E+10 | 1.8E+10 |
| 1.2E+12 | 1.0E+11 | 7.3E+10 | 5.8E+10 | 6.7E+10 | 4.5E+10 | 4.2E+10 | 1.4E+11 | 3.9E+10 | 0.0E+00 | 6.3E+10 | 1.3E+10 |
| 1.5E+12 | 9.2E+10 | 4.3E+10 | 7.6E+09 | 7.1E+10 | 6.4E+10 | 6.7E+10 | 1.6E+11 | 2.7E+10 | 7.1E+10 | 6.7E+10 | 1.4E+10 |

**Table 2.** Dose - response data for BV2 transport study with FM 4-64 labeled BME.

| Concentration (BME/mL) | Uptake fluorescence (10,000 cells x 45 min) | | | | | | | | | Mean | SEM |
|---|---|---|---|---|---|---|---|---|---|---|---|
| 0.0E+00 | 0.0E+00 | 0.0E+00 | 0.0E+00 | 0.0E+00 | 0.0E+00 | 0.0E+00 | 0.0E+00 | 0.0E+00 | 0.0E+00 | 0.0E+00 | 0.0E+00 |
| 3.0E+11 | 8.0E+10 | 0.0E+00 | 0.0E+00 | 6.6E+10 | 0.0E+00 | 2.6E+10 | 5.0E+10 | 1.0E+11 | 5.0E+10 | 4.2E+10 | 1.3E+10 |
| 6.0E+11 | 1.0E+11 | 0.0E+00 | 2.4E+10 | 1.3E+11 | 4.8E+09 | 3.9E+10 | 6.4E+10 | 5.5E+10 | 1.1E+10 | 4.8E+10 | 1.5E+10 |
| 1.2E+12 | 1.1E+11 | 7.5E+09 | 3.5E+10 | 7.4E+10 | 4.1E+10 | 2.9E+10 | 1.0E+11 | 9.6E+10 | 8.0E+10 | 6.3E+10 | 1.2E+10 |
| 1.5E+12 | 8.9E+10 | 4.3E+10 | 3.2E+10 | 5.8E+10 | 3.4E+10 | 6.1E+10 | 7.2E+10 | 5.2E+10 | 5.5E+10 | 5.5E+10 | 6.0E+09 |

**Table 3.** Time course data for bEnd.3 transport study with FM 4-64 labeled BME.

| Minutes | Uptake fluorescence (10,000 cells) | | | | | | | | | Mean | SEM |
|---|---|---|---|---|---|---|---|---|---|---|---|
| 0 | 0.0E+00 | 0.0E+00 | 0.0E+00 | 0.0E+00 | 0.0E+00 | 0.0E+00 | 0.0E+00 | 0.0E+00 | 0.0E+00 | 0.0E+00 | 0.0E+00 |
| 15 | 8.0E+09 | 8.0E+10 | 0.0E+00 | 1.3E+09 | 2.1E+10 | 0.0E+00 | 0.0E+00 | 2.1E+10 | 0.0E+00 | 1.5E+10 | 8.7E+09 |
| 30 | 1.0E+10 | 1.0E+11 | 4.0E+09 | 1.5E+10 | 2.1E+10 | 2.3E+10 | 0.0E+00 | 0.0E+00 | 0.0E+00 | 1.9E+10 | 1.0E+10 |
| 60 | 4.0E+09 | 1.0E+11 | 5.0E+10 | 2.1E+10 | 2.1E+10 | 1.5E+10 | 0.0E+00 | 4.1E+10 | 0.0E+00 | 2.8E+10 | 1.1E+10 |
| 90 | 4.0E+09 | 9.4E+10 | 8.0E+09 | 2.1E+10 | 1.1E+10 | 3.7E+10 | 0.0E+00 | 9.0E+10 | 2.1E+10 | 3.2E+10 | 1.2E+10 |
| 120 | 1.0E+10 | 1.1E+11 | 4.0E+09 | 3.7E+10 | 3.7E+10 | 1.1E+10 | 0.0E+00 | 1.3E+11 | 2.8E+10 | 4.1E+10 | 1.6E+10 |

| | | | | | | | | | | | |
|---|---|---|---|---|---|---|---|---|---|---|---|
| 240 | 2.8E+10 | 1.1E+11 | 2.2E+10 | 3.7E+10 | 5.1E+10 | 4.9E+10 | 1.2E+11 | 1.4E+11 | 1.2E+11 | 7.5E+10 | 1.5E+10 |
| 360 | 8.0E+10 | 9.0E+10 | 1.5E+11 | 1.2E+11 | 1.2E+11 | 1.1E+11 | 4.1E+10 | 1.7E+11 | 2.4E+11 | 1.2E+11 | 1.9E+10 |

**Table 4.** Time course data for BV2 transport study with FM 4-64 labeled BME.

| Minutes | Uptake fluorescence (10,000 cells) | | | | | | | | | Mean | SEM |
|---|---|---|---|---|---|---|---|---|---|---|---|
| 0 | 0.0E+00 | 0.0E+00 | 0.0E+00 | 0.0E+00 | 0.0E+00 | 0.0E+00 | 0.0E+00 | 0.0E+00 | 0.0E+00 | 0.0E+00 | 0.0E+00 |
| 15 | 3.5E+10 | 5.0E+10 | 4.0E+10 | 0.0E+00 | 5.3E+10 | 0.0E+00 | 0.0E+00 | 1.1E+11 | 0.0E+00 | 3.2E+10 | 1.2E+10 |
| 30 | 6.4E+10 | 1.1E+11 | 5.0E+10 | 4.3E+10 | 1.7E+11 | 1.9E+10 | 0.0E+00 | 1.4E+11 | 0.0E+00 | 6.6E+10 | 2.0E+10 |
| 60 | 0.0E+00 | 5.5E+10 | 2.6E+10 | 4.8E+10 | 8.2E+10 | 4.8E+09 | 0.0E+00 | 1.5E+11 | 0.0E+00 | 4.0E+10 | 1.7E+10 |
| 90 | 6.0E+10 | 1.1E+11 | 0.0E+00 | 0.0E+00 | 3.9E+10 | 2.4E+10 | 2.9E+09 | 1.6E+11 | 0.0E+00 | 4.4E+10 | 1.9E+10 |
| 120 | 7.4E+10 | 1.3E+11 | 1.1E+11 | 5.8E+10 | 1.2E+11 | 3.9E+10 | 2.9E+10 | 1.5E+11 | 0.0E+00 | 7.9E+10 | 1.7E+10 |
| 240 | 2.0E+11 | 1.8E+11 | 1.5E+11 | 6.3E+10 | 6.8E+10 | 5.3E+10 | 2.9E+10 | 1.7E+11 | 1.2E+10 | 1.0E+11 | 2.4E+10 |
| 360 | 1.5E+11 | 1.6E+11 | 1.4E+11 | 1.3E+11 | 1.2E+11 | 2.0E+11 | 1.0E+11 | 8.8E+10 | 2.1E+11 | 1.4E+11 | 1.4E+10 |

**Table 5.** TEER values for co-culture experiments.

| Days | TEER (Ohm x $cm^2$) | | | | | | | | | Mean | SEM |
|---|---|---|---|---|---|---|---|---|---|---|---|
| 1 | 11.5 | 11.0 | 14.2 | 13.9 | 12.0 | 13.4 | 15.7 | 12.8 | 14.1 | 13.2 | 0.5 |
| 2 | 20.4 | 24.5 | 20.5 | 19.7 | 18.6 | 20.0 | 21.4 | 20.7 | 22.7 | 21.0 | 0.6 |
| 3 | 25.0 | 25.8 | 30.9 | 31.2 | 28.5 | 29.7 | 29.3 | 30.3 | 29.5 | 28.9 | 0.7 |
| 4 | 32.7 | 28.5 | 36.2 | 35.9 | 34.4 | 34.9 | 34.5 | 31.4 | 32.7 | 33.5 | 0.8 |
| 5 | 34.1 | 37.0 | 35.1 | 36.4 | 34.9 | 36.4 | 31.2 | 31.7 | 31.8 | 34.3 | 0.7 |

**Table 6.** TEER values for mono-culture experiments.

| Days | TEER (Ohm x $cm^2$) | | | | | | | Mean | SEM |
|---|---|---|---|---|---|---|---|---|---|
| 1 | 10.5 | 10.5 | 15.5 | 15.3 | 11.9 | 13.4 | 12.1 | 12.8 | 0.8 |
| 2 | 23.8 | 23.3 | 21.0 | 22.0 | 18.3 | 21.2 | 19.4 | 21.3 | 0.8 |
| 3 | 21.7 | 25.8 | 28.1 | 26.2 | 23.9 | 25.0 | 21.7 | 24.6 | 0.9 |
| 4 | 17.0 | 21.5 | 22.0 | 24.5 | 19.4 | 20.7 | 17.5 | 20.4 | 1.0 |
| 5 | 16.9 | 22.4 | 18.9 | 19.6 | 15.7 | 17.8 | 13.7 | 17.8 | 1.1 |

| | | | | | | | | | |
|---|---|---|---|---|---|---|---|---|---|

**Table 7.** Dose-dependent relationship for miR-34a transfected BME in transwell studies.

| Concentration (BME/mL) | $6 \times 10^{11}$ | $1.2 \times 10^{12}$ | $2.4 \times 10^{12}$ |
|---|---|---|---|
| Permeability coefficient | 3.0E-06 | 2.8E-06 | 1.1E-06 |
| | 3.7E-06 | 2.5E-06 | 1.3E-06 |
| | 5.3E-06 | 2.3E-06 | 1.3E-06 |
| | 7.1E-06 | 2.4E-06 | 8.8E-07 |
| | 7.2E-06 | 2.5E-06 | 9.5E-07 |
| | 4.9E-06 | 2.3E-06 | 9.1E-07 |
| Mean | 5.2E-06 | 2.5E-06 | 1.1E-06 |
| SEM | 7.0E-07 | 8.2E-08 | 7.5E-08 |

**Table 8.** Time-dependent relationship for miR-34a transfected BME in transwell studies.

| Minutes | 15.0 | 30.0 | 45.0 | 60.0 |
|---|---|---|---|---|
| miRNA fluorescence | 15.7 | 15.6 | 14.7 | 22.1 |
| | 10.1 | 7.5 | 17.1 | 26.0 |
| | 10.9 | 28.3 | 30.2 | 37.8 |
| | 7.5 | 23.0 | 22.7 | 26.6 |
| | 44.5 | 40.5 | 54.3 | 44.6 |
| | 9.7 | 25.7 | 36.9 | 38.2 |
| | 14.0 | 16.3 | 12.8 | 31.0 |
| | 16.3 | 15.4 | 10.7 | 21.7 |
| | 14.5 | 10.6 | 8.8 | 18.1 |
| Mean | 15.7 | 15.6 | 14.7 | 22.1 |
| SEM | 10.1 | 7.5 | 17.1 | 26.0 |

**Table 9.** Time-dependent relationship for miR-34a transfected BME in transwell studies (Pc values).

| Minutes | 15.0 | 30.0 | 45.0 | 60.0 |
|---|---|---|---|---|
| Pc coefficient | 5.6E-06 | 2.8E-06 | 1.7E-06 | 2.2E-06 |
| | 3.2E-06 | 9.1E-07 | 2.3E-06 | 2.9E-06 |
| | 3.7E-06 | 6.6E-06 | 4.8E-06 | 4.6E-06 |
| | 1.9E-06 | 5.2E-06 | 3.4E-06 | 3.1E-06 |
| | 1.8E-05 | 7.9E-06 | 7.3E-06 | 4.4E-06 |
| | 1.8E-06 | 3.5E-06 | 3.6E-06 | 2.8E-06 |
| | 5.4E-06 | 3.3E-06 | 1.6E-06 | 3.7E-06 |
| | 5.6E-06 | 2.6E-06 | 1.0E-06 | 2.0E-06 |

| | | | | |
|---|---|---|---|---|
| | 5.7E-06 | 1.8E-06 | 8.5E-07 | 1.9E-06 |
| Mean | 5.6E-06 | 3.9E-06 | 2.9E-06 | 3.1E-06 |
| SEM | 1.6E-06 | 7.7E-07 | 6.9E-07 | 3.3E-07 |

**Table 10.** MTT cell viability tests for bEnd.3 administered FM 4-64 labeled BME.

| Concentration (BME/mL) | Control | $1.5 \times 10^{11}$ | $3 \times 10^{11}$ | $6 \times 10^{11}$ | $1.2 \times 10^{12}$ | $1.8 \times 10^{12}$ | $2.4 \times 10^{12}$ |
|---|---|---|---|---|---|---|---|
| % viability | 102.2 | 83.4 | 77.9 | 74.0 | 81.8 | 86.5 | 91.2 |
| | 94.4 | 98.3 | 104.6 | 77.9 | 86.5 | 72.4 | 106.9 |
| | 83.4 | 95.2 | 81.8 | 106.9 | 106.1 | 73.2 | 74.0 |
| | 95.9 | 115.6 | 142.2 | 103.0 | 123.4 | 88.1 | 81.8 |
| | 90.5 | 102.2 | 82.6 | 79.5 | 87.3 | 92.0 | 59.9 |
| | 133.6 | 147.7 | 77.1 | 94.4 | 64.6 | 81.8 | 65.4 |
| | 77.3 | 70.9 | 55.7 | 61.6 | 81.7 | 84.8 | 77.3 |
| | 88.4 | 59.1 | 84.5 | 102.3 | 101.0 | 108.5 | 102.3 |
| | 134.2 | 63.2 | 99.0 | 76.1 | 98.5 | 125.8 | 106.4 |
| Mean | 100.0 | 92.8 | 89.5 | 86.2 | 92.3 | 90.4 | 85.0 |
| SEM | 6.8 | 9.3 | 8.0 | 5.3 | 5.7 | 5.7 | 5.9 |

**Table 11.** MTT cell viability tests for BV2 administered FM 4-64 labeled BME.

| Concentration (BME/mL) | Control | $1.5 \times 10^{11}$ | $3 \times 10^{11}$ | $6 \times 10^{11}$ | $1.2 \times 10^{12}$ | $1.8 \times 10^{12}$ | $2.4 \times 10^{12}$ |
|---|---|---|---|---|---|---|---|
| % viability | 104.8 | 117.1 | 91.1 | 93.0 | 107.2 | 105.8 | 67.5 |
| | 98.2 | 81.2 | 108.1 | 108.1 | 106.7 | 87.3 | 61.3 |
| | 102.9 | 97.7 | 91.1 | 90.1 | 100.1 | 71.7 | 64.6 |
| | 98.7 | 108.1 | 122.8 | 69.8 | 113.8 | 168.6 | 75.0 |
| | 94.4 | 92.0 | 113.3 | 84.0 | 95.4 | 81.6 | 82.1 |
| | 101.0 | 123.7 | 116.6 | 75.5 | 116.6 | 80.7 | 82.1 |
| | 112.4 | 78.8 | 82.1 | 86.5 | 97.4 | 84.8 | 77.4 |
| | 96.8 | 105.8 | 82.1 | 67.1 | 43.4 | 65.0 | 77.6 |
| | 90.8 | 121.9 | 109.8 | 124.2 | 103.6 | 69.6 | 71.8 |
| Mean | 100.0 | 102.9 | 101.9 | 88.7 | 98.2 | 90.6 | 73.3 |
| SEM | 2.1 | 5.6 | 5.1 | 6.1 | 7.2 | 10.5 | 2.5 |